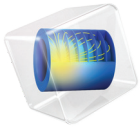

Metal Processing Module

User's Guide

6.4

COMSOL

Metal Processing Module User's Guide

Version: COMSOL 6.4

Contact Information

Visit the Contact COMSOL page at www.comsol.com/contact to submit general inquiries or search for an address and phone number. You can also visit the Worldwide Sales Offices page at www.comsol.com/contact/offices for address and contact information.

If you need to contact Support, an online request form is located on the COMSOL Access page at www.comsol.com/support/case. Useful links:

- Support Center: www.comsol.com/support
- Product Download: www.comsol.com/product-download
- Product Updates: www.comsol.com/product-update
- COMSOL Blog: www.comsol.com/blogs
- Discussion Forum: www.comsol.com/forum
- Events: www.comsol.com/events
- COMSOL Video Gallery: www.comsol.com/videos
- Support Knowledge Base: www.comsol.com/support/knowledgebase
- Learning Center: www.comsol.com/support/learning-center

Part number: CM025001

Contents

Chapter 1: Introduction

Chapter 2: Metal Processing Modeling

Chapter 3: Metal Processing Theory

Chapter 4: Metal Phase Transformation

Chapter 5: Austenite Decomposition

Chapter 6: Alpha–Beta Phase Transformation

Chapter 7: Carburization

Chapter 8: Multiphysics Interfaces and Couplings

1 Introduction

This guide describes the Metal Processing Module, an optional add-on package for the COMSOL Multiphysics® simulation software. The module is designed to perform transient analyses of processes involving metallurgical (solid-solid) phase transformations in, mainly, steels. This chapter introduces you to the capabilities of the Metal Processing Module and includes a summary of the physics interfaces and where you can find the documentation.

In this chapter:

About the Metal Processing Module

In this section:

What Can the Metal Processing Module Do?

The Metal Processing Module can be used to model different physical phenomena related to heat treatment of metals. Using this module, you can study how metallurgical phase transformations change the microstructure of a metallic material during a heating or cooling process. One example is the quenching of automotive steel transmission components, where the resulting microstructure is tailored to meet specific demands on strength and durability. Other examples include the study of phase transformations that occur during additive manufacturing of metal components and phase transformations in the heat-affected zone during welding.

There are several physics interfaces in the Metal Processing Module:

- The *Metal Phase Transformation* interface for studying diffusive and displacive metallurgical phase transformations in materials like steels.
- The *Austenite Decomposition* interface for specifically studying the cooling of steel from an austenitic state.
- The *Austenite Decomposition, Kirkaldy–Venugopalan* interface for studying the cooling of steel from an austenitic state, using the phase transformation modeling framework of Kirkaldy and Venugopalan.
- The *Austenite Decomposition, Li–Niebuhr–Meekisho–Atteridge* interface for studying the cooling of steel from an austenitic state, using the phase transformation modeling framework of Li, Niebuhr, Meekisho, and Atteridge.
- The *Alpha-Beta Phase Transformation* interface for specifically studying thermal transients in α-β titanium alloys.
- The *Carburization* interface for studying the heat treatment process of carburization.
- The *Heat Transfer with Phase Transformations* interface for modeling thermal processes involving metallurgical phase transformations.

- The *Steel Quenching* interface for modeling coupled thermal and mechanical processes involving metallurgical phase transformations.
- The *Induction Hardening* interface for modeling coupled thermal, mechanical and electromagnetic processes involving metallurgical phase transformations.

Throughout the *Metal Processing User's Guide*, the Metal Phase Transformation, the Austenite Decomposition physics interfaces, and the Alpha-Beta Phase Transformation physics interfaces are collectively referred to as *phase transformation* physics interfaces.

The physics interfaces in the Metal Processing Module can be added from the Model Wizard's **Select Physics** page under **Heat Transfer** > **Metal Processing**. The physics interfaces can also be added by right-clicking a **Component** node and selecting **Add Physics**.

Where Do I Access the Documentation and Application Libraries?

ACCESSING THE METAL PROCESSING MODULE DOCUMENTATION

The Metal Processing Module feature information, including theory and modeling details, is included in the *Metal Processing Module User's Guide*.

When you install COMSOL Multiphysics, the documentation sets are installed in several locations, both on your computer and most easily accessible while you are working in COMSOL Multiphysics. The next section details where to access it.

ACCESSING COMSOL DOCUMENTATION AND APPLICATION LIBRARIES

A number of online resources have more information about COMSOL, including licensing and technical information. The electronic documentation, topic-based (or context-based) help, and the Application Libraries are all accessed through the COMSOL Desktop.

!	If you are reading the documentation as a PDF file on your computer, the blue links do not work to open an application or content referenced in a different guide. However, if you are using the Help system in COMSOL Multiphysics, these links work to open other modules, application examples, and documentation sets.

THE DOCUMENTATION AND ONLINE HELP

The *COMSOL Multiphysics Reference Manual* describes the core physics interfaces and functionality included with the COMSOL Multiphysics license. This book also has instructions on how to use COMSOL Multiphysics and how to access the electronic Documentation and Help content.

Opening Topic-Based Help

The Help window is useful as it is connected to the features in the COMSOL Desktop. To learn more about a node in the Model Builder, or a window on the Desktop, click to highlight a node or window, then press F1 to open the Help window, which then displays information about that feature (or click a node in the Model Builder followed by the **Help** button (?). This is called *topic-based* (or *context) help*.

Win	To open the **Help** window: • In the **Model Builder**, **Application Builder**, or **Physics Builder**, click a node or window and then press F1. • On any toolbar (for example, **Home**, **Definitions**, or **Geometry**), hover the mouse over a button (for example, **Add Physics** or **Build All**) and then press F1. • From the **File** menu, click **Help** (?). • In the upper-right corner of the COMSOL Desktop, click the **Help** (?) button.

Opening the Documentation Window

Win	To open the **Documentation** window: • Press Ctrl+F1. • From the **File** menu, select **Help** > **Documentation** ( ).

THE APPLICATION LIBRARIES WINDOW

Each model or application includes documentation with the theoretical background and step-by-step instructions to create a model or application. The models and applications are available in COMSOL Multiphysics as MPH files that you can open for further investigation. You can use the step-by-step instructions and the actual models as templates for your own modeling. In most models, SI units are used to

describe the relevant properties, parameters, and dimensions, but other unit systems are available.

Once the Application Libraries window is opened, you can search by name or browse under a module folder name. Click to view a summary of the model or application and its properties, including options to open it or its associated PDF document.

	The Application Libraries Window in the *COMSOL Multiphysics Reference Manual.*

Opening the Application Libraries Window

To open the **Application Libraries** window ( ):

Win	From the **File** menu, select **Application Libraries**. To include the latest versions of model examples, from the **File** > **Help** menu select ( ) **Update COMSOL Application Libraries**.

Mac Linux	From the **File** or **Windows** menu, select **Application Libraries**. To include the latest versions of model examples, from the **Help** menu select ( ) **Update COMSOL Application Libraries**.

CONTACTING COMSOL BY EMAIL

For general product information, contact COMSOL at info@comsol.com.

COMSOL ACCESS AND TECHNICAL SUPPORT

To receive technical support from COMSOL for the COMSOL products, please contact your local COMSOL representative or send your questions to support@comsol.com. An automatic notification and a case number will be sent to you by email. You can also access technical support, software updates, license information, and other resources by registering for a COMSOL Access account.

COMSOL ONLINE RESOURCES

COMSOL website	www.comsol.com
Contact COMSOL	www.comsol.com/contact
COMSOL Access	www.comsol.com/access
Support Center	www.comsol.com/support
Product Download	www.comsol.com/product-download
Product Updates	www.comsol.com/product-update
COMSOL Blog	www.comsol.com/blogs
Discussion Forum	www.comsol.com/forum
Events	www.comsol.com/events
COMSOL Application Gallery	www.comsol.com/models
COMSOL Video Gallery	www.comsol.com/videos
Learning Center	www.comsol.com/support/learning-center
Support Knowledge Base	www.comsol.com/support/knowledgebase

Overview of the User's Guide

TABLE OF CONTENTS AND INDEX

To help you navigate this guide, see the Contents and Index sections.

MODELING WITH THE METAL PROCESSING MODULE

The Metal Processing Modeling chapter discusses how to model different problems involving phase transformations. The content covers the topics Selecting Physics Interfaces, Study Types, Modeling Phase Transformations, Defining Multiphysics Models, Selecting Discretizations, and Using Effective Material Properties.

METAL PROCESSING THEORY

The Metal Processing Theory chapters outlines the theory for the interfaces present in the Metal Processing Module. The chapter covers the topics Metallurgical Phase Transformations, Compound Material Properties, Phase Transformation Strains, Phase Transformation Latent Heat, and Carburization.

THE METAL PHASE TRANSFORMATION INTERFACE

The Metal Phase Transformation chapter describes the Metal Phase Transformation interface and its feature nodes.

THE AUSTENITE DECOMPOSITION INTERFACE

The Austenite Decomposition chapter describes the Austenite Decomposition interface and how it is based on the Metal Phase Transformation interface.

THE AUSTENITE DECOMPOSITION, KIRKALDY–VENUGOPALAN INTERFACE

The Austenite Decomposition, Kirkaldy–Venugopalan interface chapter describes how to model austenite decomposition using the phase transformation modeling framework of Kirkaldy and Venugopalan.

THE AUSTENITE DECOMPOSITION, LI–NIEBUHR–MEEKISHO–ATTERIDGE INTERFACE

The Austenite Decomposition, Li–Niebuhr–Meekisho–Atteridge interface chapter describes how to model austenite decomposition using the phase transformation modeling framework of Li, Niebuhr, Meekisho, and Atteridge.

THE ALPHA-BETA PHASE TRANSFORMATION INTERFACE

The Alpha-Beta Phase Transformation chapter describes the Alpha-Beta Phase Transformation interface, and how it is based on the Metal Phase Transformation interface.

THE CARBURIZATION INTERFACE

The Carburization chapter describes the Carburization interface and its feature nodes.

MULTIPHYSICS INTERFACES AND COUPLINGS

The Multiphysics Interfaces and Couplings chapter describes two multiphysics interfaces found under the Metal Processing branch when adding a physics interface:

- The Heat Transfer with Phase Transformations interface combines a Metal Phase Transformation interface with a Heat Transfer in Solids interface. The coupling of the interfaces appears on a domain level, where produced latent heat from the (temperature-dependent) phase transformations gives rise to a heat source in the heat equation. Optionally, phase-composition-dependent thermal material properties can be used in the heat transfer analysis.
- The Steel Quenching Interface combines an Austenite Decomposition interface with a Heat Transfer in Solids interface and a Solid Mechanics interface. There are two domain level multiphysics couplings: In the first coupling, produced latent heat from the (temperature-dependent) phase transformations gives rise to a heat source in the heat equation. In the second coupling, phase transformation strains that result from thermal expansion or transformation-induced plasticity (TRIP) are transferred to the Solid Mechanics interface as inelastic strain contributions for the computation of stresses. In the case of plasticity, the coupling also involves equivalent plastic strains and hardening functions. Optionally, phase-composition-dependent thermal and mechanical properties can be used in the heat transfer and solid mechanics analyses.
- The Induction Hardening Interface combines an Austenite Decomposition interface with a Heat Transfer in Solids interface, a Solid Mechanics interface, and a Magnetic Fields interface. There are three domain level multiphysics couplings: In the first coupling, produced latent heat from the (temperature-dependent) phase transformations gives rise to a heat source in the heat equation. In the second coupling, phase transformation strains that result from thermal expansion or transformation-induced plasticity (TRIP) are transferred to the Solid Mechanics interface as inelastic strain contributions for the computation of stresses. In the case of plasticity, the coupling also involves equivalent plastic strains and hardening functions. In the third coupling, resistive heating from the magnetic fields are added

as a heat source term in the heat equation. Optionally, phase-composition-dependent thermal, mechanical, and electromagnetic properties can be used in the heat transfer, solid mechanics, and magnetic fields analyses.

- The Phase Transformation Latent Heat multiphysics coupling adds the latent heat that is produced during phase transformations, as a heat source term, to the heat equation in a Heat Transfer interface.
- The Phase Transformation multiphysics coupling adds the transformation strains that are produced during phase transformations, as an inelastic strain contribution, to the equation for stress in a Solid Mechanics interface. The coupling also transfers stresses and the equivalent plastic strain from a Solid Mechanics interface to the coupled phase transformation interface.

2

Metal Processing Modeling

The goal of this chapter is to show you how to model different problems involving phase transformations in steels and how to include various physical phenomena that may be relevant in specific situations.

In this chapter:

Selecting Physics Interfaces

The Metal Processing Module contains six basic physics interfaces and two multiphysics interfaces. The basic physics interfaces are:

- Metal Phase Transformation — For modeling general metallurgical phase transformations.
- Austenite Decomposition — For modeling the specific case of austenite decomposing into a combination of destination phases, on cooling.
- Austenite Decomposition, Kirkaldy–Venugopalan — For modeling the specific case of austenite decomposing into a combination of destination phases, on cooling. The interface is built upon the phase transformation models of Kirkaldy and Venugopalan.
- Austenite Decomposition, Li–Niebuhr–Meekisho–Atteridge — For modeling the specific case of austenite decomposing into a combination of destination phases, on cooling. The interface is built upon the phase transformation models of Li, Niebuhr, Meekisho, and Atteridge.
- Alpha–Beta Phase Transformation — For modeling phase transformations in α–β titanium alloys.
- Carburization — For modeling carburization; the process by which carbon from a surrounding carbon rich environment diffuses into a component.

Metal Phase Transformation

The Metal Phase Transformation interface provides a basic way to model phase transformations in metals. Six common models for phase transformations in for example steels are provided. The Leblond–Devaux, the Johnson–Mehl–Avrami–Kolmogorov (JMAK), the Kirkaldy–Venugopalan, simplified, the Microstructure based, and the Hyperbolic rate models are used to model time-dependent (diffusion-controlled) phase transformations, such as the transformation of austenite into pearlite during steel hardening. In contrast, the Koistinen–Marburger model is used to model the transformation of austenite into martensite, where the amount of undercooling below the so-called martensite start temperature controls the formation of martensite. In addition to these seven types of phase transformations, you can define your own phase transformation models and let them coexist with other active phase transformations in your analysis. You can use an arbitrary number of phase

transformations in a model. The Metal Phase Transformation interface lets you generate a compound material whose properties are phase-composition-dependent. This material can be used by other physics interfaces, such as Solid Mechanics and Heat Transfer in Solids.

- Modeling Phase Transformations
- Metallurgical Phase Transformations

Austenite Decomposition

The Austenite Decomposition interface is a specialized interface that considers hardening of steel from an austenitic state. During hardening of steels, the material is heated above the austenitizing temperature. It is then cooled, and depending on the rate of cooling, a combination of destination phases such as ferrite, pearlite, bainite, and martensite can form. The Austenite Decomposition interface automatically creates corresponding **Phase** nodes and **Phase Transformation** nodes. You can also define an arbitrary number of additional phases and phase transformations. Optionally, you can define your own phase transformation models and let them coexist with other active phase transformations in the analysis. The Austenite Decomposition interface lets you generate a compound material whose properties are phase-composition-dependent. This material can be used by other physics interfaces, such as Solid Mechanics and Heat Transfer in Solids.

- Modeling Phase Transformations
- Metallurgical Phase Transformations

Austenite Decomposition, Kirkaldy–Venugopalan

The Austenite Decomposition, Kirkaldy–Venugopalan interface is a specialized version of the Austenite Decomposition interface, and additionally creates a **Steel Composition** node that is configured to define phase transformation functions and transformation temperatures according to the Kirkaldy–Venugopalan modeling framework for austenite decomposition. The created **Phase Transformation** nodes are configured to use the phase transformation functions and transformation temperatures defined by the **Steel Composition** node.

Austenite Decomposition, Li–Niebuhr–Meekisho–Atteridge

The Austenite Decomposition, Li–Niebuhr–Meekisho–Atteridge interface is analogous to the Austenite Decomposition, Kirkaldy–Venugopalan interface. The difference is that the **Steel Composition** and the **Phase Transformation** nodes are configured to represent the modeling framework of Li, Niebuhr, Meekisho, and Atteridge, for austenite decomposition.

Alpha–Beta Phase Transformation

The Alpha–Beta Phase Transformation interface is a specialized interface that is used to model phase transformations in α–β titanium alloys, such as Ti–6Al–4V. These alloys find uses in welding as well as additive manufacturing. In these applications, the material typically undergoes both heating and cooling, and depending on the rates at which this happens, different fractions of beta phase and alpha phases can form. The Alpha–Beta Phase Transformation interface automatically creates phase nodes and phase transformation nodes. In addition, transformation conditions are imposed the phase transformation nodes to, for example, restrict phase transformations to cooling or heating. The Alpha–Beta Phase Transformation interface lets you generate a compound material whose properties are phase-composition-dependent. This material can be used by other physics interfaces, such as Solid Mechanics and Heat Transfer in Solids.

- Modeling Phase Transformations
- Metallurgical Phase Transformations

Carburization

The Carburization interface provides a way to model the heat treatment process of carburization. The process involves placing a component in a carbon rich environment, at an elevated temperature. Over time, carbon is transferred into the surface of the component, and then progresses to the interior via diffusion. You can specify the carbon potential (the carbon concentration of the surrounding environment) as a function of time, to emulate a particular process. Or, you can use a simplified boost-diffuse carburization cycle that is provided by the interface. You can model the mass transfer of carbon into the surface of the component in different ways. You can prescribe the carbon concentration at the surface, or use a convective, thermally

activated carbon mass transfer. Additionally, you can model selective carburization by prescribing zero carbon flux in certain regions of the component surface.

Study Types

Metallurgical Phase transformations are inherently time dependent. Phase transformations are defined by a set of ordinary differential equations in time. The Carburization interface solves the time-dependent diffusion of carbon in a component. The only study type for the Metal Processing physics interfaces is therefore Time Dependent. In a multiphysics model involving magnetic fields, study types such as Frequency–Transient may be relevant, in which phase transformations are still handled as time dependent.

In the *COMSOL Multiphysics Reference Manual*:

- Time Dependent
- Frequency-Transient
- Studies and Solvers

Modeling Phase Transformations

This section describes how to model metallurgical solid-solid phase transformations. When you simulate processes such as hardening of steel, these phase transformations are fundamental because they ultimately determine the final properties of the material. In the phase transformation interfaces, each phase transformation is defined by a certain evolution equation that defines the time rate of change of the algebraic proportion of a destination phase at the expense of a source phase. In the following, the two modeling concepts of phases and phase transformations are discussed.

Metallurgical Phases

When you model phase transformations in a material, each transformation defines how a source phase transforms into a destination phase as a function of time. When you create a metallurgical phase node, you have to define its initial phase fraction. This is the value from which the phase fraction evolves during the analysis.

You have the option, at the physics interface level, to compute effective thermal, electromagnetic, and mechanical properties for the compound material. If you have opted to do this, you also need to define the corresponding properties of each phase. At each phase node, you can choose to create a component-level phase material. This material can be populated with properties that define the behavior of the phase. As an alternative, you can use imported material properties. This is described in Importing Material Properties and Phase Transformation Data.

The phase material properties are averaged (phase-fraction averaged) into effective material properties of a compound material that can be used in other physics interfaces. This is described in Using Effective Material Properties.

Phase Transformations

When you have created a phase transformation node, you have to choose a source phase and a destination phase. These are the two phases that are fundamentally involved in the phase transformation. You also have the option of specifying additional source phases that contribute to the formation of the destination phase. The selected phase transformation model defines the underlying type of phase transformation. They are described below.

THE LEBLOND–DEVAUX MODEL

Phase transformations in steels are based on diffusion of carbon, and the Leblond–Devaux phase transformation model is suitable to model this. You can choose between four formulations for the model — **General coefficients**, **Time and equilibrium**, **TTT diagram data**, and **Parameterized TTT diagram**. The first and second formulations require generally temperature-dependent functions that determine the characteristics of the phase transformation. The functions will be different for different phase transformations. The **TTT diagram data** formulation requires information that can be extracted from a TTT diagram, namely the time it takes at each temperature to reach a specified relative phase fraction. Typically, you would choose the transformation start line (for example, 1%). The **Parameterized TTT diagram** formulation is used to input three points from a TTT diagram, and let COMSOL Multiphysics construct a simplified TTT diagram using these points and additional curve shape parameters. The constructed TTT diagram is used internally to calculate the required parameters for the phase transformation model.

The Leblond–Devaux Model

THE JOHNSON–MEHL–AVRAMI–KOLMOGOROV (JMAK) MODEL

You can choose between five formulations for the model — **Time, equilibrium, and exponent**; **TTT diagram data**; **TTT diagram data, fixed exponent**; **Parameterized TTT diagram**; and **Parameterized TTT diagram, fixed exponent**. The first formulation can be viewed as a generalization of the **Time and equilibrium** form of the Leblond–Devaux model. In addition to the generally time-dependent functions describing the equilibrium phase fraction and the time constant, a time-dependent exponent is used. The exponent is called the Avrami exponent, and it alters the characteristic of the phase transformation. The **TTT diagram data** and **TTT diagram data, fixed exponent formulations** require information that can be extracted from the curves in a TTT diagram, namely the time it takes at each temperature to reach a specified relative phase fraction. The former requires two times to calculate the time constant and the Avrami exponent, at two respective relative phase fractions. These can represent, for example the transformation start (for example, 1%) and finish (for example, 90%) times, at each temperature. The **TTT diagram data, fixed exponent** formulation requires that you specify the Avrami exponent separately, and then use a single transformation time, such as the transformation start. The **Parameterized TTT diagram** and **Parameterized TTT diagram, fixed exponent** formulations are used to input points from a TTT diagram, and

let COMSOL Multiphysics construct a simplified TTT diagram using these points and additional curve shape parameters. The constructed TTT diagram is used internally to calculate the required parameters of the phase transformation model. In the former, two TTT curves are used. These can represent, for example, the start and finish curves of the transformation. In the latter, a single TTT curve is used to internally calculate the time constant, and the Avrami exponent is specified separately.

The Johnson–Mehl–Avrami–Kolmogorov (JMAK) Model

THE KIRKALDY–VENUGOPALAN, SIMPLIFIED MODEL

This phase transformation model is suitable for diffusion-based phase transformations, such as occur in steels during quenching. You can choose between three formulations for the model — **Rate coefficient**, **TTT diagram data**, and **Parameterized TTT diagram**. The first formulation requires a rate coefficient that represents a lumped effect of temperature and chemical composition on the rate equation for the phase transformation. The **TTT diagram data** formulation requires information that can be extracted from a TTT diagram, namely the time it takes at each temperature to reach a given relative phase fraction. This information is then used internally to calculate the required parameters for the phase transformation model. The **Parameterized TTT diagram** formulation is used to input three points from a TTT diagram, and let COMSOL Multiphysics construct a simplified TTT diagram using these points and additional curve shape parameters. The constructed TTT diagram is used internally to calculate the required parameters for the phase transformation model.

The Kirkaldy–Venugopalan, Simplified Model

THE MICROSTRUCTURE BASED MODEL

This phase transformation model is used to model austenite decomposition according to the phase transformation modeling framework of Kirkaldy and Venugopalan, and that of Li, Niebuhr, Meekisho, and Atteridge. It is most naturally used in conjunction with the **Steel Composition** node, where information of, for example, chemical

composition, is used to define phase transformation functions and transformation temperatures, that are used in the phase transformation model definition.

The Microstructure Based Model

THE KOISTINEN–MARBURGER MODEL

This phase transformation model is suitable to model the displacive martensitic transformation in steel, on rapid cooling. You can choose between two formulations for the model — **Koistinen-Marburger coefficient** and **Martensite finish temperature**. In the first formulation, you specify the **Martensite start temperature** M_s and, if applicable, select **Stress-dependent start temperature**. Then specify the **Koistinen–Marburger coefficient** β. The martensite start temperature defines the onset of the phase transformation, and the Koistinen–Marburger coefficient defines how rapidly the phase transformation progresses as the temperature decreases. The martensite start temperature M_s can be experimentally obtained from dilatometry experiments. If the integrated form of the phase transformation model is used (Equation 3-24), a value for the **Koistinen-Marburger coefficient** β can be correlated to the temperature at which the martensitic transformation is considered complete (see, for example, Ref. 9). In the second formulation, the phase transformation is defined by the **Martensite start temperature** M_s and, if applicable, select **Stress-dependent start temperature**. Then specify the **Martensite finish temperature** M_{90}. The latter is the temperature corresponding to 90% martensite formation, using the integrated form of the phase transformation model.

If you have selected **Stress-dependent start temperature**, you can let stresses affect the onset of the phase transformation through a shift of M_s. The start temperature is shifted depending on the pressure and the effective (von Mises) stress. Two coefficients a_1 and a_2 define the dependence of these stress quantities on the martensite start temperature.

In some situations, you may want to limit the phase fraction of austenite available for martensitic transformation. If you select **Incomplete transformation**, you can specify a **Minimum retained source phase fraction**, $\xi_{\mathrm{ret}}^{\mathrm{s}}$, to represent the amount of austenite unavailable for martensitic transformation.

The Koistinen–Marburger Model

For an example how to model phase transformations, see *Phase Transformations in a Round Bar*: Application Library path **Metal_Processing_Module/Tutorial_Examples/phase_transformations_in_a_round_bar**.

THE HYPERBOLIC RATE MODEL

This phase transformation model can be used for example to model dissolution of α phase in titanium, on heating. The model assumes that the rate of formation of the destination phase is inversely proportional to the phase fraction of the destination phase.

The Hyperbolic Rate Model

THE LINEAR MODEL

This phase transformation model can be used to model for example austenitization of steels. It is a simple model that assumes that the rate of formation of the destination phase is proportional to the heating rate, between a lower temperature limit T_{l}, and an upper temperature limit T_{u}.

The Linear Model

THE ODDY–MCDILL–KARLSSON MODEL

This phase transformation model is suitable for heating of hypoeutectoid steels. It was developed to model the formation of a eutectoid austenite fraction through the dissolution of carbides. Its mathematical form is based on the Johnson–Mehl–Avrami–Kolmogorov (JMAK) model, but with a specific form for the time constant in the

expression, and the equilibrium phase fraction replaced by the eutectoid fraction of austenite.

The Oddy–McDill–Karlsson Model

Calibration of Phase Transformation Models

During a thermal transient, a material point may undergo varying rates of cooling and heating. During this transient, several phase transformations can be active at the same time. This suggests that it is difficult to calibrate phase transformation models individually, as they tend to affect one another. For example, in the case of austenite decomposition, it is common in practice to present the complicated nature of phase transformations as continuous cooling transformation (CCT) or time-temperature transformation (TTT) diagrams; see Figure 2-1 and Figure 2-2 for schematic examples. Both diagrams show the start temperatures for the formation of a small fraction of different phases (F_s for the start temperature of ferrite, and so on). The fraction can be chosen arbitrarily but is often 0.1% or 1%. The difference between the two diagram types, as their names imply, is the following:

- A CCT diagram is constructed by performing experiments where a small specimen is cooled at a specified, constant, *temperature rate*.
- A TTT diagram is constructed by performing experiments where a small specimen is rapidly cooled to a temperature T_0 that is subsequently kept constant.

One method to measure the actual start temperatures required to draw each diagram is to use dilatometry experiments. Metallurgical phase transformations are accompanied by a change in volume, owing to the density difference between phases. In a dilatometer, a specimen is cooled (or heated), and its length is monitored. The specimen length will change according to basic thermal expansion, but phase transformations will induce additional length changes that can be measured.

In a real quenching situation, it is clear that material points do not experience either of the two extremes represented by the CCT and TTT diagrams (constant temperature rate versus constant temperature). Nevertheless, because experimentally obtained CCT and TTT diagrams are very common in the heat treatment community, phase transformation models must in practice be calibrated using them.

It is here useful to examine one formulation of the Leblond–Devaux model:

$$\dot{\xi}^{d} = \frac{\xi^{d}_{eq} - \xi^{d}}{\tau_{s \to d}}$$

In this equation, the phase fraction for the destination phase tends toward an equilibrium value ξ^{d}_{eq}, and the rate at which this occurs is characterized by the time constant $\tau_{s \to d}$. Note here that the equilibrium phase fraction and the time constant are in general both temperature dependent, and that temperature in turn varies with time. At constant temperature, the equation can be integrated analytically, giving

$$\xi^{d} = \xi^{d}_{eq}\left(1 - \exp\left(-\frac{t}{\tau_{s \to d}}\right)\right)$$

The equilibrium phase fraction can be deduced from an (equilibrium) iron–carbon diagram (Ref. 1) or from dilatometry experiments at a very low temperature rate (or at constant temperature after a rapid temperature drop). If we know this equilibrium phase fraction at a given temperature t_1, we can compute the temperature-dependent time constant from knowing the time it takes to reach a specific phase fraction (isothermally):

$$\tau_{s \to d} = -\frac{t_1}{\ln\left(1 - \frac{\xi^{d}}{\xi^{d}_{eq}}\right)}$$

Alternatively, if we know the time to reach, for example, 1% of the equilibrium phase fraction, that is, the *relative* phase fraction

$$X = \frac{\xi^{d}}{\xi^{d}_{eq}}$$

the time constant is obtained without knowing the equilibrium phase fraction. Thus, a TTT diagram showing curves of transformation times corresponding to relative phase fractions X can straightforwardly be used to compute the temperature-dependent time constant. In this sense, a TTT diagram is easier to use for phase transformation model calibration than a CCT diagram. This method to the calibration of phase transformation models to TTT diagram data can be used also for the Johnson–Mehl–Avrami–Kolmogorov (JMAK) and Kirkaldy–Venugopalan models. It should be pointed out that given a set of phase transformation model parameters, it is straightforward to *compute* both types of diagrams and to adjust the model parameters based on comparisons of the computed diagrams and experimental

information. It is sometimes necessary to iterate in this manner to find a sufficiently accurate set of model parameters.

As a final alternative to performing the calibration using TTT or CCT diagrams, you can import computed phase transformation data. This is described in Importing Material Properties and Phase Transformation Data.

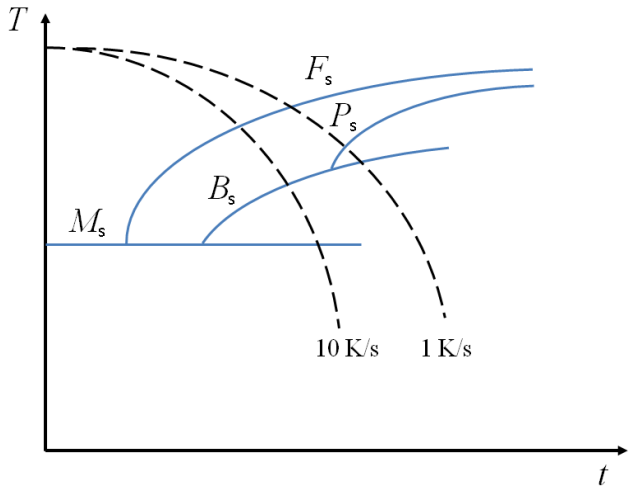

Figure 2-1: A CCT diagram showing how phases appear during cooling at two different rates. The temperatures corresponding to 1% formed fraction of ferrite, pearlite, and bainite are shown. The martensite start temperature is shown as a straight line. The time is shown on a logarithmic axis.

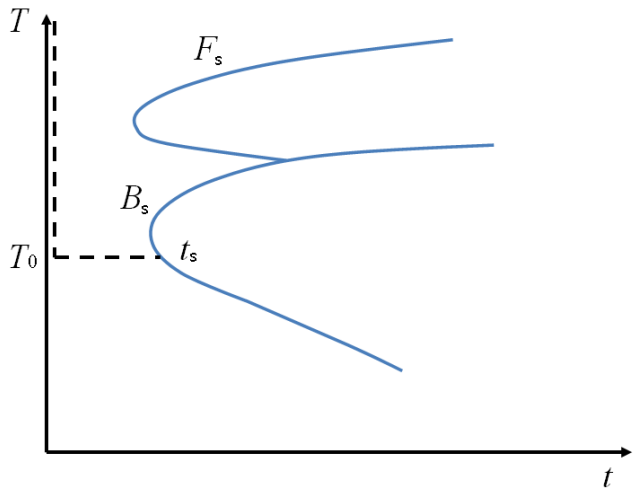

Figure 2-2: A TTT diagram showing how the temperature is rapidly decreased to a fixed value T_0 and then kept constant.

	For an example how to compute CCT and TTT diagrams, see *Transformation Diagram Computation*: Application Library path **Metal_Processing_Module/Transformation_Diagrams/ transformation_diagram_computation**.

	For an example how to calibrate a phase transformation model based on experimental TTT diagram data, see *Transformation Diagram Computation*: Application Library path **Metal_Processing_Module/ Transformation_Diagrams/calibration_against_ttt_data**.

Defining Multiphysics Models

This chapter describes how two couple the phase transformation interfaces to the Heat Transfer in Solids and Solid Mechanics interfaces. A good place to start reading is in Building a COMSOL Multiphysics Model in the *COMSOL Multiphysics Reference Manual*.

In this chapter:

- Heat Transfer with Phase Transformations — For modeling phase transformations coupled to heat transfer.
- Steel Quenching — For modeling the specific case of austenite decomposition coupled to heat transfer and solid mechanics.
- Induction Hardening — For modeling induction hardening processes including phase transformations in steel coupled to heat transfer, solid mechanics, and magnetic fields.
- Phase Transformation Latent Heat — A predefined unidirectional coupling that adds latent heat from phase transformations as a heat source term in the coupled heat transfer interface.
- Phase Transformation Strain — A predefined bidirectional coupling that is used to transfer strains and stresses to, and from, the coupled solid mechanics interface.

Heat Transfer with Phase Transformations

The Heat Transfer with Phase Transformations multiphysics interface combines the Metal Phase Transformation interface with the Heat Transfer in Solids interface. Phase transformations are generally temperature dependent, and this interface is a suitable starting point for modeling metallurgical phase transformations that occur during a thermal transient. Latent heat is generated during phase transformations, and the interface transfers this generated heat to the heat equation that is used by the Heat

Transfer in Solids interface, as shown in Figure 2-3. This is done using the Phase Transformation Latent Heat multiphysics coupling.

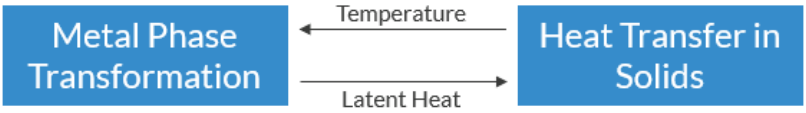

Figure 2-3: The constituent interfaces of the Heat Transfer with Phase Transformations multiphysics interface.

Steel Quenching

The Steel Quenching multiphysics interface combines the Austenite Decomposition interface with the Heat Transfer in Solids and the Solid Mechanics interfaces. It can be used to study heat treatment processes by which steel parts, which have been heated to a fully austenitic state, are quenched. The multiphysics interface couples the constituent interfaces so that effects of latent heat and phase transformation strains can be included in the analysis. Phase compositions, distortions, and residual stresses can be computed using the Steel Quenching multiphysics interface. Figure 2-4 shows how this information is passed to, and from, the Austenite Decomposition interface. Note that, for example, material properties used in Solid Mechanics can be temperature dependent, and that plastic dissipation can act as a heat source in Heat Transfer in Solids (this is not shown in Figure 2-4). The Steel Quenching multiphysics interface

uses the Phase Transformation Latent Heat multiphysics coupling and the Phase Transformation Strain multiphysics coupling.

Figure 2-4: The constituent interfaces of the Steel Quenching multiphysics interface.

For an example how to use the Steel Quenching interface, see *Carburization and Quenching of a Steel Gear*: Application Library path **Metal_Processing_Module/Steel_Quenching/carburization_and_quenching_of_a_steel_gear**.

Induction Hardening

The Induction Hardening multiphysics interface combines the Austenite Decomposition, Heat Transfer in Solids, and Solid Mechanics interfaces with the The Magnetic Fields Interface. This is the most specialized interface of the Metal Processing Module. Its purpose is to simulate the particular heat treatment process where a steel part is induction heated using a coil, and subsequently quenched. The multiphysics interface couples the constituent interfaces so that effects of latent heat, phase transformation strains, and electromagnetic heating can be included in the analysis. Figure 2-5 shows how this information is passed between the interfaces. Phase compositions, distortions, and residual stresses can be computed using the Induction Hardening multiphysics interface.

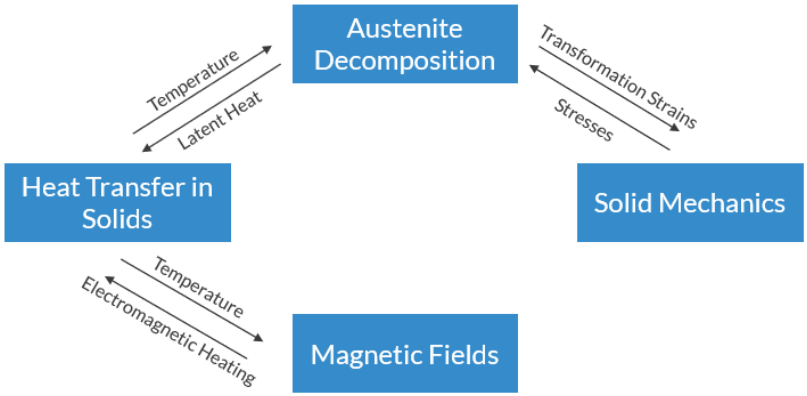

Figure 2-5: The constituent interfaces of the Induction Hardening multiphysics interface.

For cooling, the multiphysics interface is identical to the Steel Quenching multiphysics interface, but in order to model induction heating, a Magnetic Fields interface is used together with an Electromagnetic Heating multiphysics coupling.

!	Note that the Austenite Decomposition interface used in the Induction Hardening multiphysics interface does not add Phase Transformation nodes for heating. Depending on the phase composition of the steel prior to induction heating, and depending on the level of modeling detail that is warranted, one or more Phase Transformation nodes should be added to model austenitization.

Phase Transformation Latent Heat

This unidirectional multiphysics coupling generates a heat source term in the heat equation of the coupled Heat Transfer in Solids interface. The heat source term corresponds to the latent heat produced during phase transformations.

	See Phase Transformation Latent Heat in the theory chapter.

Phase Transformation Strain

This bidirectional multiphysics coupling is used to transfer strains and stresses to, and from, the coupled Solid Mechanics interface.

- If **Enable transformation-induced plasticity** is selected, the stress tensor from the Solid Mechanics interface is used to compute TRIP strains during phase transformations. These strains are used by the Solid Mechanics interface as an inelastic strain contribution.
- If **Enable thermal strains** is selected, the thermal strains are used by the Solid Mechanics interface as an inelastic contribution.

When you use this coupling, you should not use the Thermal Expansion node to compute thermal strains to be used in the Solid Mechanics interface.

- If **Enable phase plasticity** is selected, and if the **Plasticity** subnode under **Linear Elastic Material** is used by the coupled Solid Mechanics interface, the equivalent plastic strain is transferred to the phase transformation interface. This way, the individual hardening function for each phase can be evaluated.

Annealing

An **Annealing** subnode can be added to the **Phase Transformation Strain** multiphysics coupling. This subnode is used to specify an annealing temperature above which plastic hardening variables (equivalent plastic strains) are set to zero.

- The **Annealing** multiphysics subnode must be used in conjunction with the **Annealing** subnode to **Plasticity** in the coupled Solid Mechanics interface, operating on the same selection.
- TRIP strains, thermal strains, and the plastic strain tensor are unaffected by the **Annealing** subnode.

Selecting Discretization

Phase Transformation Modeling

The Metal Phase Transformation, Austenite Decomposition, and Alpha-Beta Phase Transformation interfaces provide a **Discretization for phase fractions** setting. This is used to set the shape function order for the phase fractions, and it should match the settings for the temperature field used by the Heat Transfer in Solids interface. It is set to quadratic by default, to match the default setting of the Heat Transfer in Solids interface.

Carburization Modeling

The discretization setting for Carburization interface controls the shape function order for the carbon concentration. The **Element order** is set to quadratic by default.

Using Effective Material Properties

When a material undergoes phase transformations during a thermal transient, its material properties will change. The properties are typically temperature dependent and tend to be phase dependent, too. For example, the initial yield stress at a given temperature will be higher in martensite than in ferrite — two metallurgical phases that appear during hardening of steel. When the Metal Phase Transformation, Austenite Decomposition, or Alpha-Beta Phase Transformation interface is used with Heat Transfer in Solids or Solid Mechanics, it can compute effective material properties that can be utilized by these interfaces. The benefit is that the Heat Transfer in Solids and Solid Mechanics interfaces themselves do not need to perform phase averaging of the material properties that are used.

You can generate a compound material that can be used by other physics interfaces as a domain material. The compound material is created if you use the **Create Compound Material** option at the physics interface level. This material contains effective material properties that are computed from the corresponding material properties defined for each phase.

Compound Material Properties

Note that if **Enable phase plasticity** has been selected at the physics interface level, the **User defined** option should be used for the **Isotropic hardening model** in the **Plasticity** node in Solid Mechanics.

Importing Material Properties and Phase Transformation Data

When the Metal Phase Transformation, Austenite Decomposition, Austenite Decomposition, Kirkaldy–Venugopalan, Austenite Decomposition, Li–Niebuhr–Meekisho–Atteridge, or Alpha-Beta Phase Transformation interface is used, parameters for the different phase transformations have to be defined. Additionally, if the interface is used with Heat Transfer in Solids or Solid Mechanics, the material properties of the metallurgical phases have to be defined. Phase transformations and material properties are typically temperature dependent. In the case of plasticity, the material properties also depend on plastic strain and plastic strain rate.

The effort involved in obtaining material properties and phase transformation data experimentally, or by consulting literature sources, can be time consuming and expensive. As an alternative, material properties and phase transformation data for general steels can be imported from the software JMatPro®. The following sections describe how this is done.

Material Properties

When you import material properties, one material is created for each of the metallurgical phases austenite, ferrite, pearlite, bainite, and martensite. These materials can then be used as **Phase Material** in the **Metallurgical Phase** nodes in the interfaces. In addition to material properties for the individual metallurgical phases, effective material properties that represent a compound material behavior are collected and imported into a separate material. This material can be merged into, for example, a created compound material, see Using Effective Material Properties.

To merge a material with effective properties into a compound material, use either **Merge Into** from the context menu, or use the **Merge Into** menu in the **Materials** toolbar. See Merging a Material Into Another Material for details.

LOCATION IN USER INTERFACE

Context Menu

With **Global Definitions** or a **Component** selected:

Materials > **Import Materials**

Materials > **Import Materials From**

Phase Transformation Data

When you import phase transformation data, one phase transformation node is created for each of the phase transformations involved in the decomposition of austenite:

- austenite to ferrite
- austenite to pearlite
- austenite to bainite
- austenite to martensite

In addition to data that describe the phase transformation kinetics, other data is imported and added to each phase transformation node. They are:

- phase transformation latent heat
- the transformation-induced-plasticity (TRIP) parameter

The import can be performed under the **Metal Phase Transformation**, **Austenite Decomposition**, **Austenite Decomposition, Kirkaldy–Venugopalan**, **Austenite Decomposition, Li–Niebuhr–Meekisho–Atteridge**, and **Alpha-Beta Phase Transformation** interfaces, although the **Austenite Decomposition** interface is the most natural interface to perform the import from.

- Note that you need to manually select the source phase and destination phase that participate in each imported phase transformation.
- The imported diffusive phase transformations are based on TTT data from JMatPro®, and applicable phase transformation models in COMSOL Multiphysics are configured accordingly. In addition, the imported data is processed internally into a rate contribution $A_{s \to d}$ that can be used without assuming an underlying functional form. The latter produces the best agreement across the entire range of imported data, and it uses the **User defined** phase transformation model.

LOCATION IN USER INTERFACE

Context Menu

With the **Metal Phase Transformation**, **Austenite Decomposition**, **Austenite Decomposition, Kirkaldy–Venugopalan**, **Austenite Decomposition, Li–Niebuhr–Meekisho–Atteridge**, or **Alpha-Beta Phase Transformation** interface selected:

Import Phase Transformations

Modeling Carburization

This section describes how to model the heat treatment process of carburization. The process typically involves placing a component in a carbon rich environment, and letting carbon diffuse into the component over time. When you use the Carburization interface, you need to specify the characteristics of the surrounding carburization environment, specify the way in which carbon can move across the component surface, and finally specify how carbon is able to diffuse internally in the component. This is described below.

Defining a Carburization Environment

When you use the Carburization interface, you can define the carbon concentration of the environment surrounding the component to be carburized. This is done by selecting the type of **Carburizing Cycle**. You can either specify the carbon concentration directly, as a function of time, or you can use the built-in **Boost-diffuse cycle**. In the latter situation, you use a simple cycle where the carbon potential c_{pot} is at a high value for an initial time ($t \le t_{\text{boost}}$), and after this boost period, the carbon potential is lowered, and the diffuse stage begins.

See Carbon Potential Model in the theory chapter.

Modeling Carbon Diffusion

The diffusion of carbon into a component is modeled using Fick's second law of diffusion. When you solve the carbon diffusion problem, you need to specify the initial carbon concentration in the component using the **Initial Values** node. You then need to define the diffusion coefficient to be used in the diffusion equation. This diffusion coefficient can either be specified as an expression, or specified using a provided thermally activated (Arrhenius type) form.

See Carburization in the theory chapter.

Boundary Conditions

You can model the exchange of carbon with the surrounding environment in different ways. You can apply two types boundary conditions to model the carbon mass transfer. They are of Dirichlet (prescribed carbon concentration) or of Neumann (prescribed carbon flux) types. In the case of a prescribed carbon flux, you have the option of using a thermally activated (Arrhenius type) description for the carbon mass transfer coefficient. By default, the external surfaces of a component have zero flux, which means that they do not transfer any carbon from or to the surrounding environment. The zero flux boundary conditions are replaced by the boundary conditions discussed previously. In a situation where you model selective carburization, you may want to leave parts of the external component surface with a zero carbon flux condition, as this would correspond to partially masking the surface from the surrounding environment.

See Boundary Conditions in the theory chapter.

References

1. T. Holm, P. Olsson, and E. Troell (Eds.), "Steel and its heat treatment — A handbook," *Swerea IVF,* Mölndal, 2012.

3

Metal Processing Theory

This chapter introduces you to the theory for the Metal Processing Module.

In this chapter:

Metal Phase Transformation Theory

In the following, the theory for the Metal Phase Transformation physics interface is described. This section also covers the theory for the Austenite Decomposition physics interface. These physics interfaces can be used to model metallurgical phase transformations in metals. They can be coupled to Heat Transfer in Solids and Solid Mechanics, where, for example, quenching of steel components can be performed.

Metallurgical Phase Transformations

Definitions

The material consists of a number of metallurgical phases. The fraction of each phase i is denoted ξ^i. There are in general N phases, where

$$\sum_{i=1}^{N} \xi^i = 1$$

The initial phase fraction must be defined for each phase, and the sum of initial phase fractions should be one. At the onset of an analysis, some phases may not be present, and have zero initial phase fraction.

- The phase fractions are defined in the material frame.
- Because of the employed weighting scheme for the effective mass density of the compound material, the phase fractions become algebraic fractions.
- See Compound Material Properties.

Each phase transformation describes how a source phase s transforms into a destination phase d. A phase transformation is formally defined by the rate $A_{s \to d}$ at which the destination phase d forms at the expense of the source phase s. This can be expressed as

$$A_{s \to d} = \dot{\xi}^d = -\dot{\xi}^s \tag{3-1}$$

Note that this equation describes only a single contribution to the total rates at which the destination phase forms, and the source phase decomposes. With several simultaneous phase transformations, some phases may receive more than one contribution. As an example, consider the case of three phases and two phase transformations, where phase 1 transforms into phases 2 and 3. Using the terminology above, the total rate equations for the three phases can be expressed as

$$\dot{\xi}^1 = -A_{1 \to 2} - A_{1 \to 3}$$

$$\dot{\xi}^2 = A_{1\to 2}$$

$$\dot{\xi}^3 = A_{1\to 3}$$

Note that these rate equations satisfy

$$\sum_{i=1}^{N} \dot{\xi}^i = 0$$

In COMSOL Multiphysics, a weak contribution is generated for each phase i:

$$\left(\dot{\xi}^i - \sum_j A_{j\to i}\right)\delta\xi^i$$

where the summation is done over every phase transformation for which phase j transforms into phase i. The exception to this is when all phases share the same selection as the physics interface, in which case one of the phase fractions is algebraically prescribed by the phase fractions of the other phases, and the requirement that the phase fractions add to unity.

In some situations, you may want to lump several phase transformations into one, so that several source phases decompose using the same phase transformation kinetics. One example is a simplified description of austenitization, if you are not concerned with the exact order in which phases like martensite and pearlite transform into austenite. Here, the destination phase is taken to form according to

$$\dot{\xi}^{\mathrm{d}} = A_{\mathrm{s}\to\mathrm{d}}$$

The negative of this rate is taken to be the sum of the rates of the (now several) source phases so that

$$-A_{\mathrm{s}\to\mathrm{d}} = \sum_j \dot{\xi}^j$$

where the summation is taken over the participating source phases. The contribution of each source phase to the total rate is arbitrary, and a modeling decision has to be made with regard to this indeterminacy. In COMSOL Multiphysics, the use of multiple source phases in a phase transformation is handled by assuming that each source phase rate is proportional to $-A_{\mathrm{s}\to\mathrm{d}}$ through its own current phase fraction

divided by the phase fraction sum of all participating source phases. For each source phase, the rate contribution is therefore

$$\dot{\xi}^{s} = -\xi^{s} \frac{A_{s \to d}}{\sum_{j} \xi^{j}} \tag{3-2}$$

By using Equation 3-2, the correct sum of the source phase rates is ensured, and the indeterminacy of their respective contributions is eliminated. Moreover, Equation 3-2 reduces to the standard form given by Equation 3-1 in the case of a single source phase.

Phase Transformation Models

In this section, the different types of phase transformations are described.

THE LEBLOND–DEVAUX MODEL

This phase transformation model is based on the work of Leblond and Devaux (Ref. 1). The model primarily considers carbon-diffusion-based phase transformations that occur in steels during heat treatment. Such transformations include austenite to ferrite, and austenite to bainite. There are four formulations for the Leblond–Devaux model:

- General coefficients
- Time and equilibrium
- TTT diagram data
- Parameterized TTT diagram

General coefficients

Using this form, the transformation of a source phase into a destination phase is given by

$$\dot{\xi}^{d} = K_{s \to d} \xi^{s} - L_{s \to d} \xi^{d} \tag{3-3}$$

where the phase transformation is active only when $\dot{\xi}^{d} > 0$; that is, when the right-hand side of Equation 3-3 is strictly positive. In general, the functions $K_{s \to d}$ and $L_{s \to d}$ are functions of temperature T. It was shown in Ref. 1 that the bainitic transformation additionally depends on the rate of cooling, $\dot{T}$. In this case, the functions $K_{s \to d}$ and $L_{s \to d}$ are functions of both T and $\dot{T}$.

Time and Equilibrium

This form is a special case of the general-coefficients form. The phase transformation is defined by an equilibrium phase fraction for the destination phase ξ_{eq}^{d} and a time constant $\tau_{s \to d}$. The phase transformation is given by

$$\dot{\xi}^{d} = \frac{\xi_{eq}^{d} - \xi^{d}}{\tau_{s \to d}} \tag{3-4}$$

where the phase transformation is active only when $\dot{\xi}^{d} > 0$; that is, when the right side of Equation 3-4 is strictly positive. The equilibrium phase fraction ξ_{eq}^{d} and the time constant $\tau_{s \to d}$ are typically functions of temperature.

TTT Diagram Data

At constant temperature, the time-temperature formulation of the Leblond–Devaux phase transformation model can be integrated analytically:

$$\xi^{d} = \xi_{0}^{d} + (\xi_{eq}^{d} - \xi_{0}^{d})\left(1 - \exp\left(-\frac{t}{\tau_{s \to d}}\right)\right) \tag{3-5}$$

where ξ_{0}^{d} is the initial phase fraction. This enables straightforward calibration of the model parameters from TTT diagram data. At a given temperature, and assuming that the initial phase fraction is zero, the equilibrium phase fraction of the destination phase is ξ_{eq}^{d}. A relative phase fraction of the destination phase is defined such that it is 1.0 as the equilibrium phase fraction is reached. The relative phase fraction X is given by

$$X = \frac{\xi^{d}}{\xi_{eq}^{d}} \tag{3-6}$$

In the TTT diagram in Figure 3-1, a curve representing a fixed destination phase fraction ξ_{1}^{d} is shown. At a fixed temperature T, this destination phase fraction is reached at time t_1, so that

$$\xi_{1}^{d} = \xi^{d}(t_1) \tag{3-7}$$

The characteristic time is then expressed as

$$\tau_{s \to d} = -\frac{t_1}{\ln(1 - X_1)} \tag{3-8}$$

where t_1 will vary with temperature, and the relative phase fraction X_1 is understood to be the relative phase fraction corresponding to ξ_{1}^{d}.

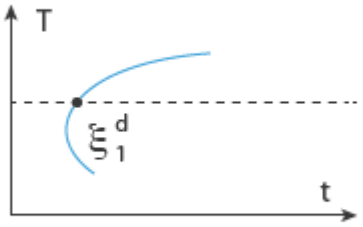

Figure 3-1: Constant phase fraction curve in a TTT diagram.

This way of fitting the Leblond–Devaux model to TTT diagram data will be most accurate near the chosen phase fraction curve in the TTT diagram. If, for example, the 0.1% curve is used, the phase transformation model will likely predict the onset of destination phase formation well, but it will show poorer agreement with the TTT diagram near completion.

Parameterized TTT Diagram

The Leblond–Devaux model can use a parameterized TTT diagram as input, in which a single TTT curve is used to identify the time constant. See Parameterized TTT Diagram.

THE JOHNSON–MEHL–AVRAMI–KOLMOGOROV (JMAK) MODEL

This phase transformation model is based on the work by Leblond and others (Ref. 4).

There are five formulations for the JMAK model:

- Time, equilibrium, and exponent
- TTT diagram data
- TTT diagram data, fixed exponent
- Parameterized TTT diagram
- Parameterized TTT diagram, fixed exponent

Time, Equilibrium, and Exponent

The first formulation can be viewed as a generalization of the time-temperature formulation for the Leblond–Devaux model. It is based on an Avrami law of the form

$$\xi^{d} = \xi_{0}^{d} + (\xi_{eq}^{d} - \xi_{0}^{d})\left(1 - \exp\left(-\left(\frac{t}{\tau_{s\to d}}\right)^{n_{s\to d}}\right)\right) \tag{3-9}$$

In the equation above, the initial phase fraction is ξ_{0}^{d}, and the equilibrium phase fraction ξ_{eq}^{d}, the time constant $\tau_{s\to d}$ and the Avrami exponent $n_{s\to d}$ are typically functions of temperature. On rate form, Equation 3-9 can be expressed as

$$\dot{\xi}^{d} = \frac{\xi_{eq}^{d} - \xi^{d}}{\tau_{s\to d}} n_{s\to d}\left(\ln\left(\frac{\xi_{eq}^{d} - \xi_{0}^{d}}{\xi_{eq}^{d} - \xi^{d}}\right)\right)^{1-\frac{1}{n_{s\to d}}} \tag{3-10}$$

where the explicit time dependence has been eliminated. The phase transformation is active only when $\dot{\xi}^{d} > 0$; that is, when the right side of Equation 3-10 is strictly positive. For the special case of $n_{s\to d} = 1$, the equation reduces to the time-and-equilibrium form of the Leblond–Devaux model (Equation 3-4). The JMAK phase transformation model in Equation 3-10 has a mathematical disadvantage in that an initial destination phase fraction equal to zero will yield a trivial zero solution, as the logarithm will evaluate to zero. There are different ways to circumvent this problem. One way is to require the initial phase fraction be assigned a small, but finite, value. Another way is to modify the rate equation itself, so that a zero initial phase fraction does not yield a trivial zero solution. In the phase transformation interfaces, the JMAK phase transformation model in Equation 3-10 is modified for phase fractions ξ^{d} in the vicinity of ξ_{0}^{d}. Below a certain threshold, the argument for the logarithm is modified so that the logarithm does not produce a zero value. This threshold phase fraction is set to 10^{-5} by default. A problem can arise in the case of nonzero initial phase fractions. Namely, if other phase transformations in the model operate such that the metallurgical phase that is the destination phase fraction above *decreases*, the JMAK model would run into problems as $\xi^{d} < \xi_{0}^{d}$, whereby the argument in the logarithm becomes negative. One way to handle this is to exclude the effect of the initial phase fraction in the rate expression in Equation 3-10. This is done

in COMSOL Multiphysics. A judgment has to be made in each situation whether this is a proper modeling assumption.

The phase fraction threshold variable used by the JMAK phase transformation model can be modified in the **Equation View** of the **Phase Transformation** node. Typically, the default value of 10^{-5} should not have to be changed.

Note that the Avrami exponent used by the JMAK phase transformation model should be greater than or equal to one. If a smaller value is encountered, it will be replaced by an exponent of one.

TTT Diagram Data

As in the case of the Leblond–Devaux model, the JMAK model can be calibrated using TTT diagram data. The integrated form in Equation 3-9 is used to calibrate the time constant $\tau_{s\to d}$ and the Avrami exponent $n_{s\to d}$. To calibrate these two phase transformation model parameters, two curves are needed from a TTT diagram; see Figure 3-2. As for the Leblond–Devaux model, a zero initial phase fraction is assumed when calibrating the JMAK model. At a fixed temperature T, the two destination phase fractions are reached at times t_1 and t_2, respectively, so that

$$\xi_1^d = \xi^d(t_1) \tag{3-11}$$

$$\xi_2^d = \xi^d(t_2) \tag{3-12}$$

After some algebra, the time constant and Avrami exponent can be expressed as

$$n_{s\to d} = \ln\left(\frac{\ln(1-X_1)}{\ln(1-X_2)}\right)/\ln\left(\frac{t_1}{t_2}\right) \tag{3-13}$$

$$\tau_{s\to d} = t_1/(-\ln(1-X_1))^{\frac{1}{n_{s\to d}}} \tag{3-14}$$

where the relative phase fractions X_1 and X_2 are understood to be the relative phase fractions corresponding to ξ_1^d and ξ_2^d, respectively. The transformation times t_1 and t_2 will vary with temperature.

Parameterized TTT Diagram

The JMAK model can use a parameterized TTT diagram as input, in which two TTT curves are used to identify the time constant and the Avrami exponent. See Parameterized TTT Diagram.

Parameterized TTT Diagram, Fixed Exponent

The JMAK model can use a parameterized TTT diagram as input, in which a single TTT curve is used to identify the time constant. Using this formulation, you specify the Avrami exponent separately. See Parameterized TTT Diagram.

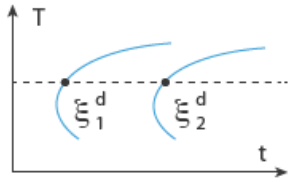

Figure 3-2: Constant phase fraction curves in a TTT diagram.

THE KIRKALDY–VENUGOPALAN, SIMPLIFIED MODEL

This phase transformation model is based on the work by Kirkaldy and Venugopalan (Ref. 11), and extended and modified by several others. There are three formulations for the Kirkaldy–Venugopalan, simplified phase transformation model:

- Rate coefficient
- TTT diagram data
- Parameterized TTT diagram

Rate Coefficient

The rate form describing the phase transformation model is given by

$$\xi^d = \xi^d_{eq}\xi^d_0 \frac{X^{\frac{2(1-X)}{3}}(1-X)^{\frac{2X}{3}}}{\exp(C_r X^2)} \tag{3-15}$$

where ξ_{eq}^{d} is the equilibrium phase fraction, $\dot{\xi}_{0}^{d}$ is a reference rate that in principle depends on temperature, chemical composition, and grain size, and C_r is a retardation coefficient. The relative phase fraction X is defined as

$$X = \frac{\xi^{d}}{\xi_{eq}^{d}} \tag{3-16}$$

so that the rate of formation of the destination phase approaches zero as the relative phase fraction approaches one; that is, when the phase transformation nears completion. The Kirkaldy–Venugopalan, simplified phase transformation model shares the mathematical disadvantage with the JMAK model in that an initial destination phase fraction of zero will yield a trivial zero solution. Similar to the JMAK phase transformation model, the Kirkaldy–Venugopalan, simplified phase transformation model is modified. A small threshold value for the destination phase fraction ξ^{d} is introduced, so that the phase transformation model produces a nonzero rate below this value.

The phase fraction threshold variable used by the Kirkaldy–Venugopalan, simplified phase transformation model can be modified in the **Equation View** of the **Phase Transformation** node. Typically, the default value of 10^{-5} should not have to be changed.

TTT Diagram Data

The Kirkaldy–Venugopalan, simplified phase transformation model can be calibrated using TTT diagram data. Similar to the cases of the Leblond–Devaux and JMAK phase transformation models, the expression for the rate of destination phase formation is used to identify the model parameters, here the rate coefficient $\dot{\xi}_{0}^{d}$. Rearranging the rate expression in Equation 3-15 gives an expression of the form

$$\dot{X} = \dot{\xi}_{0}^{d} F(X) \tag{3-17}$$

where the relative phase fraction X has been used. Note that at a fixed temperature, the equilibrium phase fraction ξ_{eq}^{d} is constant, and it can therefore be included in the rate term $\dot{X}$ in Equation 3-17. The reference rate $\dot{\xi}_{0}^{d}$ is temperature dependent (and dependent on chemical composition and grain size, in the original Kirkaldy–Venugopalan formulation. (See The Microstructure Based Model). At a fixed temperature, t_1 is the time to reach the destination phase fraction ξ_{1}^{d} (or alternatively, to reach the relative phase fraction X_1), see Figure 3-3. This is expressed as

$$\xi_1^{\mathrm{d}} = \xi^{\mathrm{d}}(t_1) \tag{3-18}$$

$$X_1 = \frac{\xi_1^{\mathrm{d}}}{\xi_{\mathrm{eq}}^{\mathrm{d}}} \tag{3-19}$$

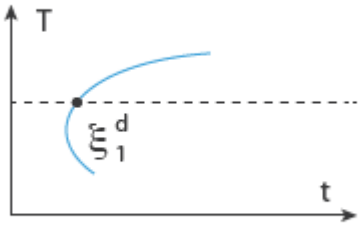

Figure 3-3: Constant phase fraction curve in a TTT diagram.

Using Equation 3-17, the rate coefficient is expressed as

$$\xi_0^{\mathrm{d}} = \frac{1}{t_1}\int_0^{X_1}\frac{\mathrm{d}g}{F(g)} = \frac{1}{t_1}\int_0^{X_1}\frac{\exp(C_{\mathrm{r}}g^2)}{g^{\frac{2(1-g)}{3}}(1-g)^{\frac{2g}{3}}}\mathrm{d}g \tag{3-20}$$

Note that if the retardation coefficient C_{r} is known, the integral can be computed *a priori* for a fixed X_1. The rate coefficient is therefore inversely proportional to the time it takes to reach the relative phase fraction X_1. The time t_1 generally depends on temperature.

Parameterized TTT Diagram

The Kirkaldy–Venugopalan, simplified model can use a parameterized TTT diagram as input, in which a single TTT curve is used to identify the rate coefficient. See Parameterized TTT Diagram.

THE MICROSTRUCTURE BASED MODEL

The rate describing the phase transformation model is given by

$$\dot{\xi}^{d} = \xi^{d}_{eq} f_G f_C f_T \left|T_u - T\right|^{m} \times \frac{X^{a(1-X)}(1-X)^{aX}}{\exp(C_r X^2)} \tag{3-21}$$

where ξ^{d}_{eq} is the equilibrium phase fraction, f_G is a function of the ASTM grain size, f_C is a function of chemical composition, and f_T is an Arrhenius term. The rate depends on the level of undercooling $|T_u - T|$ below an upper temperature limit T_u. The exponent m is an undercooling exponent. The exponent a in the rate term that alters the characteristic of the sigmoid function. The phase transformation is accompanied by the definition of a lower temperature limit T_l, below which the transformation becomes inactive. The term C_r is a retardation coefficient. The functions (grain size dependence, chemical composition dependence, and the Arrhenius term) are collected into a single function $f = f_G f_C f_T$, which, together with the undercooling term, can be interpreted as the reference rate $\dot{\xi}^{d}_{0}$ of the Kirkaldy–Venugopalan, simplified model. Note that the rate equation is dimensionally incorrect in its original formulation by Kirkaldy and Venugopalan. The equation is taken as is, with the understanding that temperature unit is Kelvin, and the resulting rate unit is one per second. The relative phase fraction X is defined as

$$X = \frac{\xi^{d}}{\xi^{d}_{eq}} \tag{3-22}$$

so that the rate of formation of the destination phase approaches zero as the relative phase fraction approaches one; that is, when the phase transformation nears completion. The sigmoid function used in the Microstructure based phase transformation model has mathematical disadvantages that it shares with the Kirkaldy–Venugopalan, simplified phase transformation model, see The Kirkaldy–Venugopalan, Simplified Model.

THE KOISTINEN–MARBURGER MODEL

This phase transformation model was developed by Koistinen and Marburger (Ref. 2) to model the diffusionless (displacive) austenite to martensite transformation in iron-carbon alloys and carbon steels. The onset of the transformation, which only occurs on cooling, is characterized by a critical start temperature — the martensite start temperature M_s. Above this temperature, no transformation from austenite (the source phase) to martensite (the destination phase) occurs. Below M_s, the amount of formed martensite is proportional to the undercooling below M_s, given by $M_s - T$. On rate form, the Koistinen–Marburger equation can be written

$$\dot{\xi}^{\mathrm{d}} = -\xi^{\mathrm{s}}\beta\dot{T} \tag{3-23}$$

where β is the Koistinen–Marburger coefficient. Note that the transformation of austenite into martensite only occurs below M_{s} and only during cooling (that is, when $\dot{T} < 0$). To make the onset of martensitic transformation numerically smooth, a parameter ΔM_s is used. The smoothing parameter defines a smoothed Heaviside function that makes the onset of martensitic transformation gradual. The parameter should be chosen small enough that the start temperature characteristic is retained. Assuming a constant cooling rate and that the phase fraction of austenite at M_{s} is ξ_0^{s}, the rate equation can be integrated to

$$\xi^{\mathrm{d}} = \xi_0^{\mathrm{s}}(1 - \exp(-\beta(M_s - T))) \tag{3-24}$$

This integrated form is commonly found in the literature. Instead of defining the Koistinen–Marburger coefficient directly, a martensite finish temperature, M_{90}, can be defined, corresponding to reaching a phase fraction of 90% using Equation 3-24, and assuming 100% initial source phase fraction. The Koistinen–Marburger coefficient β is then given by

$$\beta = -\frac{\ln 0.1}{M_s - M_{90}}$$

The rate form of Equation 3-23 is more general, and from a computational standpoint it is more suitable for implementation. The rate form is therefore used in the phase transformation interfaces.

It has been recognized that the onset of martensitic transformation can be affected by an externally applied stress. The martensite start temperature is commonly shifted by a linear combination of the externally applied hydrostatic stress and the externally applied von Mises effective stress. In Ref. 3 the shift in martensite temperature is expressed as

$$A\sigma_{\mathrm{m}} + B\sigma_{\mathrm{e}}$$

which means that the martensitic transformation will only take place if

$$T < M_{\mathrm{s}} + A\sigma_{\mathrm{m}} + B\sigma_{\mathrm{e}} = M_{\mathrm{s}} - a_1 p + a_2\sigma_{\mathrm{e}}$$

where we have used the coefficient names a_1 and a_2, and the pressure instead of the hydrostatic stress.

THE HYPERBOLIC RATE MODEL

This phase transformation model can be used for example to model dissolution of α phase in titanium, on heating. It is based on the idea that the rate of formation of a phase is inversely proportional to its phase fraction. Here, it is expressed as

$$\dot{X} = \frac{P}{X} \tag{3-25}$$

with

$$X = \frac{\xi^{\mathrm{d}}}{\xi^{\mathrm{d}}_{\mathrm{eq}}} \tag{3-26}$$

In this phase transformation model, the "equilibrium phase fraction" $\xi^{\mathrm{d}}_{\mathrm{eq}}$ does not represent a true equilibrium phase fraction in the sense that the phase transformation would saturate to this value. Nevertheless, it is used as a parameter in the definition of X, for consistency. By combining the previous two equations, the rate equation used in COMSOL Multiphysics becomes

$$\dot{\xi}^{\mathrm{d}} = (\xi^{\mathrm{d}}_{\mathrm{eq}})^2 \frac{P}{\xi^{\mathrm{d}}} \tag{3-27}$$

THE LINEAR MODEL

This phase transformation model is meant for heating conditions. It can be used to model austenitization of steels, where the full details of the phase transformation into austenite are not required. The phase transformation model is active between a lower and upper temperature limit, and its rate equation in COMSOL Multiphysics is given by

$$\dot{\xi}^{\mathrm{d}} = \frac{\dot{T}}{T_{\mathrm{u}} - T_{\mathrm{l}}} \tag{3-28}$$

for $\dot{T} > 0$. For isothermal or cooling conditions, the rate is zero. Integrating the rate equation in Equation 3-28, and using the fact that the destination phase begins to form only once the lower temperature limit T_{l} is reached, the following linear expression is obtained for the evolution of the destination phase fraction with temperature.

$$\xi^{\mathrm{d}} = \frac{T - T_{\mathrm{l}}}{T_{\mathrm{u}} - T_{\mathrm{l}}} \tag{3-29}$$

THE ODDY–MCDILL–KARLSSON MODEL

This phase transformation model was originally developed to model the dissolution of pearlite and the formation of eutectoid austenite during heating of hypoeutectoid steels. Its rate equation is of the same form as the Johnson–Mehl–Avrami–Kolmogorov phase transformation model (Equation 3-10), and it is given by

$$\xi^{\mathrm{d}} = \frac{\xi^{\mathrm{d}}_{\mathrm{eu}} - \xi^{\mathrm{d}}}{\tau_{\mathrm{s}\to\mathrm{d}}} n_{\mathrm{s}\to\mathrm{d}} \left(\ln\left(\frac{\xi^{\mathrm{d}}_{\mathrm{eu}}}{\xi^{\mathrm{d}}_{\mathrm{eu}} - \xi^{\mathrm{d}}} \right) \right)^{1 - \frac{1}{n_{\mathrm{s}\to\mathrm{d}}}} \tag{3-30}$$

where the equilibrium phase fraction of the destination phase has been replaced by the eutectoid phase fraction (of austenite) and the initial phase fraction is assumed to be zero. The time constant is given by

$$\tau_{\mathrm{s}\to\mathrm{d}} = q_1 |T - T_{\mathrm{l}}|^{-q_2} \tag{3-31}$$

and the Avrami constant, according to Oddy and others (Ref. 20) is set to $n_{\mathrm{s}\to\mathrm{d}} = 3$, and the time parameters are given by

$$q_1 = 2.06 \cdot 10^8 s$$

$$q_2 = 4.8$$

USER DEFINED

Using this option, other types of phase transformations can be defined. A user-defined phase transformation assumes that a source phase decomposes into a destination phase according to Equation 3-1.

Parameterized TTT Diagram

A curve in a TTT diagram represents the time it takes to form a certain relative phase fraction of a metallurgical phase, under isothermal conditions. Using experimental TTT diagram data, one can extract transformations times across a range of temperatures and thereby characterize temperature-dependent phase transformations. This is what you typically need to do for the TTT Diagram Data formulations of the Leblond–Devaux, the JMAK, and the Kirkaldy–Venugopalan phase transformation models. In some situations, it may be sufficient to approximate the shape of a TTT curve using analytical functions. COMSOL Multiphysics provides a functionality to enter three characteristic time-temperature points on a TTT curve, and together with

two shape parameters, construct an approximate a TTT curve. The three points that are used to define the TTT curve in this way are:

- A point on the upper part of the curve
- A point on the lower part of the curve
- The point defining the “nose” of the curve

The points are designated U (upper), L (lower), and N (nose), see Figure 3-4.

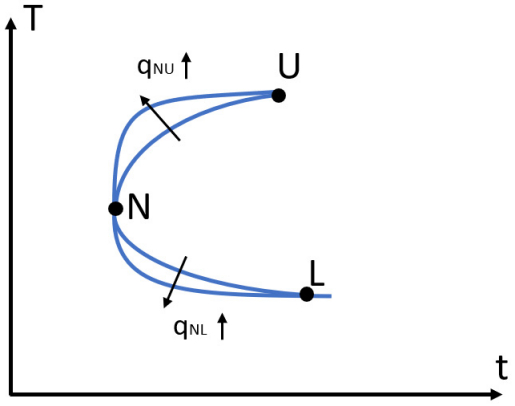

Figure 3-4: A parameterized TTT curve.

The parameterized TTT curve is defined by two analytical functions that meet at the nose. They are:

$$\log\left(\frac{t}{t_{\mathrm{N}}}\right) = \log\left(\frac{t_{\mathrm{L}}}{t_{\mathrm{N}}}\right)\left(\frac{T-T_{\mathrm{N}}}{T_{\mathrm{L}}-T_{\mathrm{N}}}\right)^{q_{\mathrm{NL}}},\ T < T_{\mathrm{N}}$$

$$\log\left(\frac{t}{t_{\mathrm{N}}}\right) = \log\left(\frac{t_{\mathrm{U}}}{t_{\mathrm{N}}}\right)\left(\frac{T-T_{\mathrm{N}}}{T_{\mathrm{U}}-T_{\mathrm{N}}}\right)^{q_{\mathrm{NU}}},\ T \geq T_{\mathrm{N}}$$

The shape parameters q_{NL} and q_{NU} are used to control the shape of the curve below the nose (NL) and above the nose (NU), and the effect of increasing them is schematically shown in Figure 3-4. A shape parameter value of two produces a quadratic function in the log time - temperature space, and so on. When you parameterize the curves in a TTT diagram in this way, COMSOL Multiphysics will internally use the TTT curves in the same way as if you had used the TTT Diagram Data formulations.

For hypoeutectoid steels that are being cooled from an austenitic state, the phase transformations into different destination phases occur across certain temperature ranges. For example, no ferrite forms before the temperature falls below the A_{e3} temperature in an Fe–C diagram, as austenite is stable above this temperature. Another example is the (eutectoid) A_{e1} temperature above which no pearlite forms. These temperatures, and other temperatures that are important when modeling phase transformations in steels, depend not only on the carbon content of the material, but also on other alloying elements. There exist several empirical models in the literature, and COMSOL Multiphysics provides several of these temperatures through the **Steel Composition** node that can be used in the Metal Phase Transformation and Austenite Decomposition interfaces. The temperatures can be readily accessed by the **Phase Transformation** nodes to facilitate phase transformation modeling.

THE AE1 AND AE3 TEMPERATURES

In an Fe–C diagram, the A_{e1} and A_{e3} temperature lines represent the lower and upper limits of the two-phase ferrite–austenite region. For a steel of a given carbon content, the A_{e3} temperature can be viewed as a ferrite start temperature, that is, the upper temperature for ferrite formation when cooling the steel from the purely austenitic state. Similarly, the A_{e1} temperature can be viewed as the pearlite start temperature, see Figure 3-5.

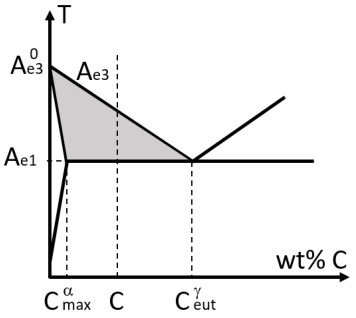

Figure 3-5: A schematic Fe–C diagram. The ferrite–austenite two-phase region is indicated in gray.

Andrews (Ref. 14) developed empirical models for these temperatures, based on the alloying elements of the material. The models are given by

$$A_{e1}(°C) = 723 - 16.9Ni + 29.1Si + 6.38W - 10.7Mn + 16.9Cr + 290As$$

$$A_{e3}(°C) = 910 - 203\sqrt{C} + 44.7Si - 15.2Ni + 31.5Mo + 104V + 13.1W - 30Mn - 11Cr - 20Cu + 700P + 400Al + 120As + 400Ti$$

where C, Si, Ni, and so forth, are the weight percentages of the respective alloying elements. These expressions are valid for steels with a carbon concentration less than 0.6% by weight. As an alternative to using the models by Andrews, you can use a parameterized description of the A_{e1} and A_{e3} temperature lines. To do this, you specify directly the A_{e3} temperature at zero carbon concentration, A_{e3}^0, the A_{e1} temperature, and the eutectoid concentration of austenite, C_{eut}^{γ}. This gives the following linear expression for the A_{e3} temperature line:

$$A_{e3} = A_{e3}^0 - \frac{A_{e3}^0 - A_{e1}}{C_{eut}^{\gamma}} \times C$$

where C is the carbon concentration of the steel. In contrast to the formulation by Andrews, the A_{e3} temperature line is here linear in the carbon concentration.

Note that the A_{e1} and A_{e3} temperature lines intersect at the eutectoid point. The models by Andrews are valid for a carbon concentration less than 0.6%, which means that the eutectoid point may be poorly estimated by these models.

THE BAINITE START TEMPERATURE

Unlike the A_{e1} and A_{e3} temperatures, the onset of bainite formation does not correspond to an equilibrium temperature in the Fe–C diagram. Nevertheless, several empirical relationships for a bainite start temperature, B_s, exist in the literature. COMSOL Multiphysics provides two models for this temperature. The model by Steven and Haynes (Ref. 15) is given by

$$B_s(°C) = 830 - 270C - 90Mn - 37Ni - 70Cr - 83Mo$$

and the bainite start temperature according to Kirkaldy and Venugopalan (Ref. 11) is given by

$$B_s(°C) = 656 - 57.7C - 75Si - 35Mn - 15.3Ni - 34Cr - 41.2Mo$$

In the expressions above, it is understood that the alloying elements are expressed in terms of their respective weight percentages.

THE MARTENSITE START TEMPERATURE

The onset of martensitic transformation is commonly represented by the martensite start temperature which is a parameter in the Koistinen–Marburger phase transformation model. COMSOL Multiphysics provides two models for the martensite start temperature. The model by Andrews (Ref. 14) is given by

$$M_s(^\circ\mathrm{C}) = 539 - 423C - 30.4Mn - 12.1Cr - 17.7Ni - 7.5Mo$$

and the model by Steven and Haynes (Ref. 15) is given by

$$M_s(^\circ\mathrm{C}) = 561 - 474C - 33Mn - 17Cr - 17Ni - 21Mo$$

In the expressions above, it is understood that the alloying elements are expressed in terms of their respective weight percentages.

Equilibrium Phase Fractions

In several of the phase transformation models in COMSOL Multiphysics, a model parameter is the equilibrium phase fraction of the destination (forming) phase, $\xi_{\mathrm{eq}}^{\mathrm{d}}$. When a hypoeutectoid steel is cooled from an austenitic state, ferrite begins to form when the temperature falls below A_{e3}.

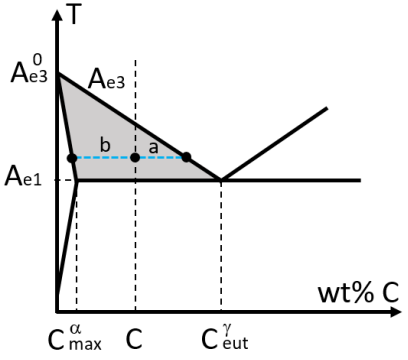

Figure 3-6: A schematic Fe–C diagram and the points involved in calculating the equilibrium phase fraction of ferrite.

In an Fe–C diagram (Figure 3-6), the equilibrium phase fraction of ferrite in this austenite–ferrite two-phase region can be extracted using a simple lever rule as

$$\xi_{\mathrm{eq}}^{\alpha} = \frac{a}{a+b}$$

Note that in using the lever rule, the ferrite region *above* the eutectoid temperature A_{e1} is taken to be a line from A_{e3}^{0} to the ferrite carbon solubility, $C_{\mathrm{max}}^{\alpha}$, at A_{e1}.

The formation of free ferrite below the eutectoid temperature A_{e1} during quenching can be included. COMSOL Multiphysics provides two models of the equilibrium phase fraction of ferrite below the eutectoid temperature, see Hippchen and others (Ref. 18) for a description. In one model, the equilibrium phase fraction of ferrite is taken to be constant below A_{e1}, and equal to the equilibrium phase fraction at A_{e1}, see Figure 3-7.

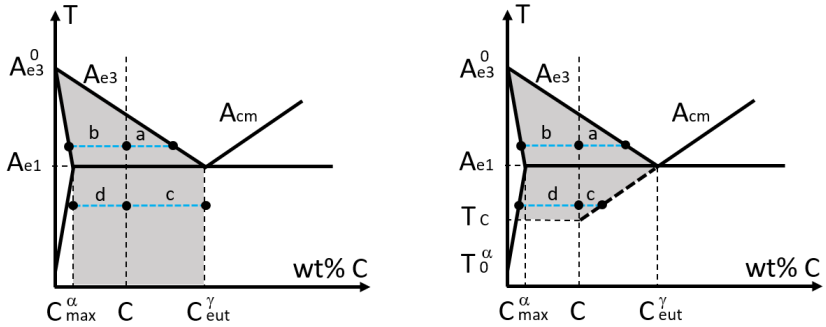

Figure 3-7: A schematic Fe–C diagram showing how the lever rule is used above and below eutectoid temperature. On the left, a constant equilibrium phase fraction of ferrite below the eutectoid. On the right, the Hultgren extrapolation is used.

In the other model, the equilibrium phase fraction of ferrite is computed by considering a modified Fe–C diagram. The A_{cm} line in the Fe–C diagram is extrapolated according to Hultgren (Ref. 19). The lever rule is employed using this extrapolated line to compute the equilibrium phase fraction, see Figure 3-7. The equilibrium phase fraction of ferrite below the eutectoid temperature in the two models can be expressed as

$$\xi_{eq}^{\alpha} = \frac{c}{c+d}$$

Note that in using the lever rule, the ferrite region *below* the eutectoid temperature A_{e1} is taken to be a line from T_0^{α} to the ferrite carbon solubility, C_{max}^{α}, at A_{e1}.

To model the formation of pearlite and bainite below the eutectoid temperature, the corresponding equilibrium phase fractions are taken to be

$$\xi_{eq}^{p} = \xi_{eq}^{b} = 1 - \xi_{eq}^{\alpha}$$

Phase Transformation Functions

The Microstructure based phase transformation model uses information deriving from, for example, grain size and chemical composition. Kirkaldy and Venugopalan (Ref. 11) expressed a set of phase transformation functions that were used to model the decomposition of austenite into ferrite, pearlite, and bainite. Based on this methodology, Li, Niebuhr, Meekisho, and Atteridge (Ref. 12) presented a similar set of phase transformation functions for the decomposition of austenite. In addition, Åkerström and Oldenburg (Ref. 13) modified the set of phase transformation functions by Kirkaldy and Venugopalan, to better capture the behavior of boron steels in press hardening applications. The general form for the phase transformations is

$$\dot{\xi}^{d} = \xi_{eq}^{d} f_G f_C f_T \left| T_u - T \right|^m \times \frac{X^{a(1-X)}(1-X)^{aX}}{\exp(C_r X^2)}$$

Overall, the following values for m, a, and C_r are

- $m = 2$ for the decomposition of austenite into bainite, and $m = 3$ otherwise.
- $a = 2/5$ for all phase transformations according to Li, Niebuhr, Meekisho, and Atteridge, and $a = 2/3$ otherwise.
- The retardation coefficient is $C_r = 0$, except where explicitly defined below.

The upper temperature limit T_u for the three phase transformations are

- $T_u = A_{e3}$ for the decomposition of austenite into ferrite.
- $T_u = A_{e1}$ for the decomposition of austenite into pearlite.
- $T_u = B_s$ for the decomposition of austenite into bainite.

AUSTENITE TO FERRITE (KIRKALDY–VENUGOPALAN)

$$f_G = 2^{\frac{G-1}{2}}$$

$$f_C = \frac{1}{59.6Mn + 1.45Ni + 67.7Cr + 244Mo}$$

$$f_T = \exp\left(-\frac{23.5\text{kcal}}{RT}\right)$$

The chemical dependence function was modified by Åkerström and Oldenburg to account for boron. In their formulation, the function is

$$f_C = \frac{1}{59.6Mn + 1.45Ni + 67.7Cr + 244Mo + 1.9 \cdot 10^5 B}$$

AUSTENITE TO PEARLITE (KIRKALDY–VENUGOPALAN)

$$f_G = 2^{\frac{G-1}{2}}$$

$$f_C = \frac{1}{1.79 + 5.42(Cr + Mo + 4MoNi)}$$

$$\frac{1}{f_T} = \exp\left(\frac{27.5\text{kcal}}{RT}\right) + (0.01Cr + 0.52Mn)\exp\left(\frac{37\text{kcal}}{RT}\right)$$

The chemical dependence function was modified by Åkerström and Oldenburg to account for boron. In their formulation, the function is

$$f_C = \frac{1}{1.79 + 5.42(Cr + Mo + 4MoNi) + 3.1 \cdot 10^3 B}$$

AUSTENITE TO BAINITE (KIRKALDY–VENUGOPALAN)

$$f_G = 2^{\frac{G-1}{2}}$$

$$f_C = \frac{10^4}{2.34 + 10.1C + 3.8Cr + 19Mo}$$

$$f_T = \exp\left(-\frac{27.5\text{kcal}}{RT}\right)$$

$$C_r = 1.9C + 2.5Mn + 0.9Ni + 1.7Cr + 4Mo - 2.6$$

AUSTENITE TO FERRITE (LI–NIEBUHR–MEEKISHO–ATTERIDGE)

$$f_G = 2^{0.41G}$$

$$f_C = \frac{1}{\exp(1 + 6.31C + 1.78Mn + 0.31Si + 1.12Ni + 2.70Cr + 4.06Mo)}$$

$$f_T = \exp\left(-\frac{27.5\text{kcal}}{RT}\right)$$

AUSTENITE TO PEARLITE (LI–NIEBUHR–MEEKISHO–ATTERIDGE)

$$f_G = 2^{0.32G}$$

$$f_C = \frac{1}{\exp(-4.25 + 4.12C + 4.36Mn + 0.44Si + 1.71Ni + 3.33Cr + 5.19\sqrt{Mo})}$$

$$f_T = \exp\left(-\frac{27.5\text{kcal}}{RT}\right)$$

AUSTENITE TO BAINITE (LI–NIEBUHR–MEEKISHO–ATTERIDGE)

$$f_G = 2^{0.29G}$$

$$f_C = \frac{1}{\exp(-10.23 + 10.18C + 0.85Mn + 0.55Ni + 0.90Cr + 0.36Mo)}$$

$$f_T = \exp\left(-\frac{27.5\text{kcal}}{RT}\right)$$

Hardness

Maynier and others (Ref. 16) have proposed a method for estimating the Vickers hardness (HV) based on the chemical composition of a steel, together with the final phase composition and the cooling rate during quenching. The Vickers hardness is calculated as a dimensionless number, although in its original definition, the unit is kgf/mm^2. The hardness number is given by a phase fraction weighted sum of the hardnesses of the individual metallurgical phases.

$$HV = (\xi^{f} + \xi^{p})HV^{f+p} + \xi^{b}HV^{b} + \xi^{m}HV^{m}$$

where the superscripts f, p, b, and m denote ferrite, pearlite, bainite, and martensite, respectively. The hardnesses of the individual phases are given by

$$\begin{aligned} HV^{f+p} &= 42 + 223C + 53Si + 30Mn + 12.6Ni + 7Cr + 19Mo \\ &+ (10 - 19Si + 4Ni + 8Cr + 130V)\log V_r \end{aligned}$$

$$\begin{aligned} HV^{b} &= -323 + 185C + 330Si + 153Mn + 65Ni + 144Cr + 191Mo \\ &+ (89 + 53C - 55Si - 22Mn - 10Ni - 20Cr - 33Mo)\log V_r \end{aligned}$$

$$HV^{m} = 127 + 949C + 27Si + 11Mn + 8Ni + 16Cr + 21\log V_r$$

where the hardnesses of ferrite and pearlite are taken to be equal. In the expressions above, the term V_r is the cooling rate, expressed in K/h, as the temperature passes 700 degrees Celsius during cooling, and C, Si, Ni, and so forth, are the weight percentages of the respective alloying elements.

Based on the calculated Vickers Hardness, the Rockwell C hardness (HRC), applicable to nonaustenitic steels, is calculated in accordance with (Ref. 17) as

$$HRC = 31.49 + 7.96683 \times 10^{-2}HV - 3.55432 \times 10^{-5}HV^{2} - \frac{6.72816 \times 10^{3}}{HV}$$

Compound Material Properties

The material consists of a mixture of metallurgical phases, each with a phase fraction that is evolving during the analysis. When the Metal Processing Module is used together with the Heat Transfer in Solids and Solid Mechanics interfaces, it is of interest to compute effective material properties so that a compound material can be defined and used by these physics interfaces. This chapter describes how various thermal and mechanical properties are averaged in terms of the phase fractions of the material.

Heat Transfer Properties

The thermal conductivity and mass density of the compound material are computed using linear weighting by the phase fractions. The properties are given by

$$k = \sum_{i=1}^{N} \xi^i k^i$$

$$\rho = \sum_{i=1}^{N} \xi_0^i \rho_0^i$$

Note that the mass density of the compound material is computed using the initial phase fraction ξ_0^i and the density evaluated at the volume reference temperature, $\rho_0^i = \rho^i(T_{\mathrm{ref}}^i)$. This is necessary, because a temperature-dependent compound material density of a body defined on the material frame would violate mass conservation. In addition to the compound material density, a current density can also be defined as

$$\rho_{\mathrm{th}} = \sum_{i=1}^{N} \xi^i \rho^i .$$

This density is used internally by the physics interface to compute thermal strains, but it is not used as a material property of the compound material.

The thermal conductivity of the compound material uses a full tensor description. The heat capacity at constant pressure is computed by using a linear weighting of the volumetric heat capacity ρC_p, having already computed ρ:

$$C_p = \frac{1}{\rho}\sum_{i=1}^{N} \xi^i \rho^i C_p^i \text{ ..}$$

If geometric nonlinearity is used, k and ρC_p are convected to the spatial frame in the Heat Transfer in Solids physics interface.

Electromagnetic Properties

The relative permeability, the electric conductivity, and the relative permittivity for the compound material are computed using a linear weighting by the phase fractions. The properties are given by

$$\mu_r = \sum_{i=1}^{N} \xi^i \mu_r^i \tag{3-32}$$

$$\sigma = \sum_{i=1}^{N} \xi^i \sigma^i \tag{3-33}$$

$$\varepsilon_r = \sum_{i=1}^{N} \xi^i \varepsilon_r^i \tag{3-34}$$

The electromagnetic properties for the compound material use a full tensor description.

Mechanical Properties

The mechanical properties for the compound material are generally computed using linear weighting by the phase fractions. The exception is in the case where phase plasticity is modeled, where other types of weighting schemes can be used for the initial yield strength of the compound material.

ELASTICITY

The elastic behavior of the compound material is assumed to be isotropic and defined by a linear weighting of the Young's moduli and Poisson's ratios of the phases. This is reasonable because the elastic properties for the different phases are similar at a given temperature.

$$E = \sum_{i=1}^{N} \xi^i E^i$$

$$\nu = \sum_{i=1}^{N} \xi^i \nu^i$$

PLASTICITY

It is not obvious what weighting scheme should be used to define an effective initial yield strength because the initial yield strengths of the phases will differ. The following weighting scheme is used:

$$\sigma_{ys0} = \sum_{i=1}^{N} g_i(\xi^i)\sigma_{ys0}^i$$

The simplest model for the initial yield strength of the compound material uses a linear weighting

$$g_i(\xi^i) = \xi^i$$

This scheme is reasonable when the initial yield strengths are similar. However, it is well known that the yield strength of some metallurgical phases can differ significantly. Most notably, martensite is typically an order of magnitude harder than austenite, and a linear mixture rule is unsuitable. Geijselaers (Ref. 8) developed a weighting scheme that is suitable in this situation. In this model, it is assumed that the hardest phase is considerably harder than the softest phase. Assuming that the hard phase is m and the soft phase is γ, the Geijselaers weighting scheme is given by

$$g_i(\xi^i) = \begin{cases} \xi^i, & i \neq m \\ f_i(\xi^i), & i = m \end{cases}$$

with

$$f_m(\xi^m) = \xi^m(C + 2(1-C)\xi^m - (1-C)(\xi^m)^2)$$

$$C = 1.383\frac{\sigma_{ys0}^{\gamma}}{\sigma_{ys0}^{m}}$$

The hardening function for the compound material is defined using the linear weighting

$$\sigma_h = \sum_{i=1}^{N} \xi^i \sigma_h^i(\varepsilon_{pe}^i) \tag{3-35}$$

where ε_{pe}^i is the equivalent plastic strain of the phase.

EQUIVALENT PLASTIC STRAINS

In Equation 3-35, the hardening function for each individual phase depends on equivalent plastic strain. If we denote the equivalent plastic strain of the compound material ε_{pe}, we must define how the equivalent of each phase ε_{pe}^i evolves with this strain. The simplest assumption is to use the evolution equation

$$\dot{\varepsilon}_{pe}^i = \dot{\varepsilon}_{pe}$$

which is to say that the equivalent plastic strain of phase *i* follows that of the compound material. If phase transformation and mechanical straining occur simultaneously, the equivalent plastic strain of the diminishing source phase of the phase transformation can be taken to follow that of the compound material, and this is the behavior in the phase transformation physics interfaces. However, for a phase which is increasing in fraction during plastic straining, this assumption is questionable. Leblond (Ref. 7) derived an evolution equation for the equivalent plastic strain, which is suitable for the forming destination phase. The evolution equations for the source and destination phases are

$$\dot{\varepsilon}_{pe}^s = \dot{\varepsilon}_{pe}$$

$$\dot{\varepsilon}_{pe}^d = \dot{\varepsilon}_{pe} - \frac{\dot{\xi}^d}{\xi^d}(\varepsilon_{pe}^d - \Theta_{s\to d}\varepsilon_{pe}^s)$$

where the plasticity memory coefficient $\Theta_{s \to d}$ was introduced to model that some plastic straining present in the source phase at the instant of transformation will be carried over to the forming destination phase. A zero plasticity memory coefficient means that no plastic straining will be remembered.

Phase Transformation Strains

We consider two types of strains that appear during a thermal transient involving metallurgical phase transformations. These strains originate from:

- Thermal expansion
- Transformation-induced plasticity (TRIP)

Other inelastic strains may also be present during a thermal transient, such as plastic strains or creep strains.

Thermal Expansion

It is well known that different metallurgical phases occupy different volumes at a given temperature. For example, when austenite transforms into martensite, the thermal contraction due to cooling is accompanied by a volumetric expansion when the martensite begins to form. There are two formulations for computing thermal strains in the compound material. The strain based formulation uses a phase fraction weighted sum of the thermal strains of each phase. The density based formulation uses the change in density during temperature changes and phase transformations.

STRAIN BASED FORMULATION

In the strain based formulation, the thermal strain of the compound material is given by

$$\varepsilon_{\text{th}} = \sum_{i=1}^{N} \xi^i \varepsilon_{\text{th}}^i$$

In this equation, the thermal strains of the individual phases are computed using a secant thermal expansion model, requiring a coefficient of thermal expansion and a strain volume reference temperature for each phase.

Consider the simple case where phase 1 transforms into phase 2. In 1D, the thermal strain is

$$\varepsilon_{\text{th}} = \xi^I \alpha^I(T)(T - T^I_{\text{ref}}) + \xi^{II} \alpha^{II}(T)(T - T^{II}_{\text{ref}})$$

where $\alpha(T)$ and T_{ref} are the secant coefficient of thermal expansion and strain volume reference temperature, for the respective phases I and II. Figure 3-8 shows the thermal

strain. For simplicity, the coefficients of thermal expansion for the two phases in the figure are constant (but different). In the figure, a fictitious phase transformation has been used to illustrate when phase *I* transforms completely into phase *II* as the temperature is lowered. No separate volumetric term is required to model this type of phase transformation strain, as it is included in the definition of the thermal expansion itself.

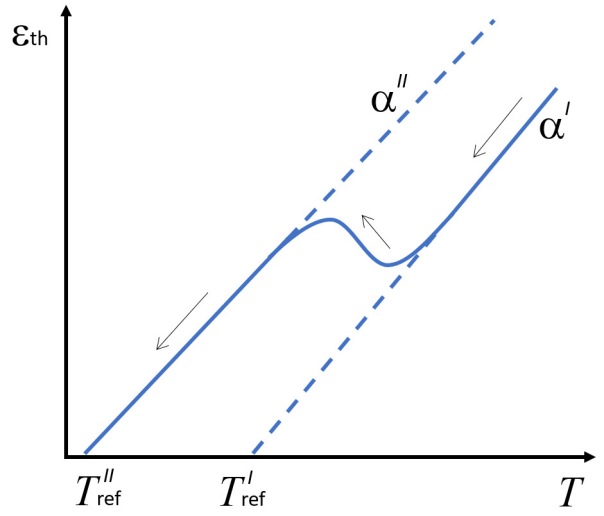

Figure 3-8: The strain based formulation for thermal strains.

DENSITY BASED FORMULATION

Instead of expressing thermal strain contributions from each phase separately, this formulation uses the temperature-dependent densities and the evolving phase composition to express a volumetric strain. To compute a reference density, the initial phase composition and the densities evaluated at their respective volume reference temperature are used. The evolving thermal volumetric strain is then given by

$$\varepsilon_{th} = \frac{\rho}{\rho_{th}} - 1 = \frac{\sum_{i=1}^{N} \xi_0^i \rho_0^i}{\sum_{i=1}^{N} \xi^i \rho^i} - 1 = \frac{\sum_{i=1}^{N} \xi_0^i \rho^i(T_{ref}^i)}{\sum_{i=1}^{N} \xi^i \rho^i(T)} - 1$$

Consider, as in the previous section, a case of two phases, where one transforms into the other as the temperature decreases. Initially, this fictitious material consists entirely of phase *I*. The volume reference temperature for phase *I* is equal to the initial temperature, so that the thermal strain is zero at this temperature. As the temperature decreases, the density of the compound material is exactly equal to the evolving density of phase *I*. As the phase transformation takes place, the compound material density changes both with temperature and the changing phase composition. Finally, phase *I* has transformed fully into phase *II*, and the compound material density becomes identical to the density of phase *II* on further reduction in temperature, see Figure 3-9.

For the density based formulation, two points should be made:

- The choice of volume reference temperature for a given phase i is inconsequential if $\xi_0^i = 0$.
- If different volume reference temperatures are specified for phases that are present initially, unexpected volumetric strains can result.

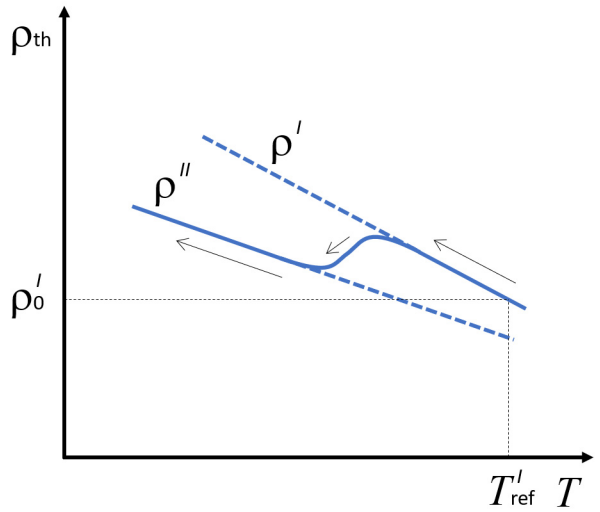

Figure 3-9: The density based formulation for thermal strains.

Transformation-Induced Plasticity

Plastic strains in metals result from deviatoric stresses that exceed the yield strength of the material. However, during phase transformations, inelastic strains may appear already at smaller stress levels. This transformation-induced plasticity (TRIP) is therefore different from classical plasticity in that it does not involve a yield criterion and that it appears at stress levels that would otherwise be insufficient to cause plastic straining even in the softest of the phases. A description of TRIP strain rate, common in the literature (see, for example, Ref. 4), is

$$\dot{\varepsilon}_{\mathrm{tp,\,s\to d}} = \frac{3}{2} K^{\mathrm{TRIP}}_{\mathrm{s\to d}} \cdot \frac{\mathrm{d}\Phi(\xi^{\mathrm{d}})}{\mathrm{d}\xi^{\mathrm{d}}} \dot{\xi}^{\mathrm{d}} \cdot \mathrm{dev}(S)$$

where the strain rate is proportional to the deviatoric part of the second Piola–Kirchhoff stress tensor S through the transformation-induced-plasticity parameter $K^{\mathrm{TRIP}}_{\mathrm{s\to d}}$, the derivative of the saturation function $\Phi(\xi^{\mathrm{d}})$, and the rate of formation of the destination phase $\dot{\xi}^{\mathrm{d}}$. Values for the transformation-induced-plasticity parameter $K^{\mathrm{TRIP}}_{\mathrm{s\to d}}$ will depend on the type of phase transformation. It can depend on, for example, carbon content and temperature (see Ref. 5). In Ref. 6, the transformation-induced-plasticity parameter for a given steel is expressed in terms of the relative volumetric thermal strain between the source and destination phases, and the yield stress of the source phase:

$$K^{\mathrm{TRIP}}_{\mathrm{s\to d}} = \frac{2\Delta\varepsilon^{\mathrm{s\to d}}_{\mathrm{th}}}{\sigma^{\mathrm{s}}_{\mathrm{ys}}}$$

The strain term in the expression above is the axial thermal strain difference between the source and destination phases. In terms of the temperature-dependent densities of the source and destination phases, this can be expressed as:

$$\Delta\varepsilon^{\mathrm{s\to d}}_{\mathrm{th}} = \frac{1}{3}\left(\frac{\rho^{\mathrm{s}}_{\mathrm{th}}}{\rho^{\mathrm{d}}_{\mathrm{th}}} - 1\right) = \frac{1}{3}\left(\frac{\rho^{\mathrm{s}}(T)}{\rho^{\mathrm{d}}(T)} - 1\right)$$

which gives

$$K^{\mathrm{TRIP}}_{\mathrm{s\to d}} = \frac{2}{3\sigma^{\mathrm{s}}_{\mathrm{ys}}}\left(\frac{\rho^{\mathrm{s}}_{\mathrm{th}}}{\rho^{\mathrm{d}}_{\mathrm{th}}} - 1\right) \tag{3-36}$$

Another method to represent the thermal strain difference is the to utilize coefficients of thermal expansion and volume reference temperatures of source and destination phases. This gives the alternative expression for the thermal strain difference:

$$\Delta\varepsilon_{th}^{s\to d} = \frac{1}{3}(\mathrm{tr}(\alpha^d)(T - T_{ref}^d) - \mathrm{tr}(\alpha^s)(T - T_{ref}^s))$$

Because the coefficients of thermal expansion for source and destination phases can in general be anisotropic, we use the average value of the normal components. This gives the following expression for the transformation-induced-plasticity parameter:

$$K_{s\to d}^{TRIP} = \frac{2}{3\sigma_{ys}^s}(\mathrm{tr}(\alpha^d)(T - T_{ref}^d) - \mathrm{tr}(\alpha^s)(T - T_{ref}^s)) \qquad (3\text{-}37)$$

Several propositions exist for the saturation functions; see Table 3-1 and Ref. 10. Through the user-defined option, you can define the derivative of the saturation function.

TABLE 3-1: SATURATION FUNCTIONS FOR THE TRIP STRAIN RATE.

TYPE	EXPRESSION
Abrassart	$\xi^d(3 - 2\sqrt{\xi^d})$
Desalos	$\xi^d(2\text{-}\xi^d)$
Leblond	$\xi^d(1 - \ln\xi^d))$ for $\xi^d > 0.03$, zero otherwise
Tanaka	ξ^d

The total TRIP strain rate is given by

$$\dot{\varepsilon}_{tp} = \sum_{s\to d} \dot{\varepsilon}_{tp,\, s\to d}$$

Total Strain Contribution

When thermal and TRIP strains are computed, they can be used in a Solid Mechanics interface as an inelastic strain contribution. The contributions from thermal and TRIP strains are added to form a total strain contribution. In the Solid Mechanics interface, this contribution is used additively in the case of an additive strain definition or used to form an inelastic-deformation-gradient contribution in the case of geometric nonlinearity with nonlinear strains; see Inelastic Strain Contributions. In the latter case, the contribution is used multiplicatively.

Phase Transformation Latent Heat

The heat rate Q_0 that is released during a phase transformation is characterized by the enthalpy per unit volume $\Delta H_{s \to d}$ (see Ref. 5). The heat rate that is associated with the transformation of a source phase into a destination phase can be expressed as

$$Q_0 = \Delta H_{s \to d} \xi^d \tag{3-38}$$

The heat rates that result from each phase transformation are added, and they can be used as a heat source when solving the heat equation. A weak contribution is added to the weak form of the heat equation:

$$\hat{Q}_0 \delta(T)$$

where $\hat{Q}_0$ is the sum of the contributions Q_0 from each phase transformation (Equation 3-38), and T is the temperature degree of freedom used in the Heat Transfer in Solids interface.

Carburization

Carburization is a heat treatment process where a component is placed in a carbon rich atmosphere, at an elevated temperature. During the process, carbon diffuses into the surface of the component, and the carbon concentration in the component changes with time as carbon continues to diffuse to the interior. The process of carburization is modeled using Fick's second law of diffusion. The carbon concentration c during carburization depends on position and time as $c = c(\mathbf{X},t)$, where $\mathbf{X}$ denotes material coordinates, and t is time. The carbon concentration represents the mass fraction of carbon, and it is thus dimensionless. The carbon concentration is governed by the following equation:

$$\frac{\partial c}{\partial t} + \nabla \cdot (-D\nabla c) = 0$$

where D is the diffusion coefficient, or diffusivity. The diffusivity can be specified directly, or it can be modeled using an Arrhenius expression of the form

$$D = D_0 \exp\left(-\frac{Q_\mathrm{D}}{RT}\right)$$

where D_0 is a pre-exponential factor, Q_D is an activation energy, and R is the gas constant.

Carbon Potential Model

During carburization, the carbon rich atmosphere can be changed over time to produce a desired carbon profile near the surface of the component. In COMSOL Multiphysics, you can specify the carbon potential c_pot of the surrounding atmosphere as a function of time, or you can use a boost-diffuse cycle (Figure 3-10). For the boost-diffuse cycle, the carbon potential is defined by

$$c_\mathrm{pot} = \begin{cases} c_\mathrm{boost}, & t \le t_\mathrm{boost} \\ c_\mathrm{diffuse}, & t > t_\mathrm{boost} \end{cases}$$

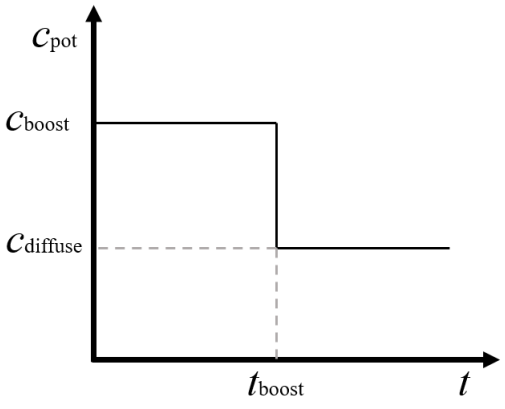

Figure 3-10: The Boost-diffuse cycle.

Boundary Conditions

When a component is subjected to an environment of different carbon concentration, carbon can diffuse into or out from its surface. This mass transfer can be modeled in two ways:

- A prescribed carbon flux (a Neumann condition): Carbon mass transfer is modeled using a convection boundary condition
- A prescribed carbon concentration (a Dirichlet condition): Carbon mass transfer is enabled by means of a prescribed value on the surface

A special case of prescribed carbon flux is the case of zero carbon flux.

PRESCRIBED CARBON FLUX

The convective mass transfer of carbon from the environment into a surface with outward normal $\mathbf{n}$ is given by

$$-\mathbf{n} \cdot (-D\nabla c) = b \cdot (c_{ext} - c)$$

where b is the mass transfer coefficient, and c_{ext} is the carbon concentration of the exterior. A natural way to define the carbon concentration of the exterior is to take it as equal to the carbon potential c_{pot} of the surrounding carburizing atmosphere. The mass transfer coefficient can be specified directly, or defined as thermally activated

$$b = b_0 \exp\left(-\frac{Q_b}{RT}\right)$$

where b_0 is a pre-exponential factor and Q_b is an activation energy. In a given situation, these quantities would have to be estimated or measured experimentally.

PRESCRIBED CARBON CONCENTRATION

A simple way to model the carbon exchange is to simply prescribe the carbon concentration at the surface of the component to be equal to the carbon concentration of the exterior. This modeling approach avoids having to characterize the carbon mass transfer, but it may instead exaggerate it because the surface will be saturated.

References

1. J.B. Leblond and J.C. Devaux, "A new kinetic model for anisothermal metallurgical phase transformations in steels including effect of austenite grain size," *Acta Metall.*, vol. 32, no. 1, pp. 137–146, 1984.

2. D.P. Koistinen and R.E. Marburger, "A general equation prescribing the extent of the austenite–martensite transformation in pure iron–carbon alloys and plain carbon steels," *Acta Metall.*, vol. 7, no. 1, pp. 59–60, 1959.

3. S. Denis, E. Aeby–Gautier, and A. Santos Simón, "*Stress–phase–transformation interactions — basic principles, modelling, and calculation of internal stresses*," *Mat. Sci. Tech.*, vol. 1, no. 10, pp. 805–814, 1985.

4. J.B. Leblond, G. Mottet, J. Devaux, and J.C. Devaux, "Mathematical models of anisothermal phase transformations in steels, and predicted plastic behaviour," *Mat. Sci. Tech.*, vol. 1, no. 10, pp. 815–822, 1985.

5. B. Liscic, H.M. Tensi, L.C.F. Canale, and G.E. Totten (Eds.), *Quenching theory and technology,* CRC Press, Taylor & Francis Group, 2010.

6. J.B. Leblond, J. Devaux, and J.C. Devaux, "Mathematical modelling of transformation plasticity in steels I: Case of ideal-plastic phases," *Int. J. Plast.*, vol. 5, pp. 551–572, 1989.

7. J.B. Leblond, "Mathematical modelling of transformation plasticity in steels II: Coupling with strain hardening phenomena," *Int. J. Plast.*, vol. 5, pp. 573–591, 1989.

8. H.J.M. Geijselaers, *Numerical simulation of stresses due to solid state transformations: The simulation of laser hardening,* doctoral dissertation, Univ. of Twente, Enschede, 2003.

9. J. Gyhlesten Back, *Modelling and characterisation of the martensite formation in low-alloyed carbon steels*, licentiate thesis, Luleå Univ. of Technology, Luleå, 2017.

10. S. Boettcher, M. Böhm, and M. Wolff, *A comprehensive model of thermo-elasto-plasticity with phase transitions in steel*, Zentrum für Technomathematik, Universität Bremen, 2013.

11. J.S. Kirkaldy and D. Venugopalan, *Phase Transformations in Ferrous Alloys*, Am, Inst. Min. Engg., Philadelphia, Pa 1984.

12. M.V. Li, D.V. Niebuhr, L.L. Meekisho, and D.G. Atteridge, "A Computational Model for the Prediction of Steel Hardenability," *Met. Mater. Trans. B*, vol. 29, pp. 661–672, 1998.

13. P. Åkerström and M. Oldenburg, "Austenite Decomposition during press hardening of a boron steel — Computer simulation and test," *J. Mat. Proc. Techn.*, vol. 174, pp. 399–406, 2006.

14. K.W. Andrews, "Empirical formulae for the calculation of some transformation temperatures," *J. Iron Steel Inst.*, vol. 203, pp. 721–727, 1965.

15. W. Steven and A.G. Haynes, "The temperature of formation of martensite and bainite in low-alloy steels," *J. Iron Steel Inst.*, vol. 183, pp. 349–359, 1956.

16. P. Maynier, B. Jungmann, and J. Dollet, *Hardenability concepts with applications to steels*, eds. D.V. Doane and J.S. Kirkaldy, The Metallurgical Society of AIME, Warrendale, PA, pp. 518–545, 1978.

17. ASTM Standard E140–2012b ε1, "Standard Hardness Conversion Tables for Metals Relationship Among Brinell Hardness, Vickers Hardness, Rockwell Hardness, Superficial Hardness, Knoop Hardness, Scleroscope Hardness, and Leeb Hardness," ASTM International, West Conshohocken, PA, 2013.

18. P. Hippchen, A. Lipp, H. Grass, P. Craighero, M. Fleischer, and M. Merklein, "Modelling kinetics of phase transformation for the indirect hor stamping process to focus on car body parts with tailored properties," *J. Mat. Proc. Techn.*, vol. 228, pp. 59–67, 2016.

19. A. Hultgren, 'Diskussion über "The physics of Hardenability" von R.F. Mehl,' *Hardenability of Alloy Steels*, pp. 55–56, 1938 (in German).

20. A.S. Oddy, J.M.J. McDill, and L. Karlsson, "Microstructural predictions including arbitrary thermal histories, reaustenitization and carbon segregation effects," Can. Metall. Quart., vol. 35, no. 3, pp. 275-283, 1996.

4

Metal Phase Transformation

This chapter describes the Metal Phase Transformation Interface ( ) and its functionality. It is found under the **Heat Transfer** > **Metal Processing** branch ( ) when adding a physics interface.

The Metal Phase Transformation Interface

The **Metal Phase Transformation** interface ( ) is found under the **Heat Transfer** > **Metal Processing** ( ) branch when adding a physics interface. The physics interface is intended for studying metallurgical phase transformations. You can use this interface to study diffusional, displacive, and user-defined (solid state) phase transformations. Physical phenomena, such as latent heat of phase transformation and transformation strains, can be computed and used in Heat Transfer in Solids and Solid Mechanics. With the Nonlinear Structural Materials Module or the Geomechanics Module, plastic strains and hardening behavior of each metallurgical phase can be used in Solid Mechanics. Different sections of the **Settings** panel will be active depending on the space dimension that the interface is used in, see Table 4-1.

TABLE 4-1: PHYSICS INTERFACE SECTIONS.

SECTION	AVAILABILITY
Material Properties	1D, 1D axisymmetric, 2D, 2D axisymmetric, 3D
Heat Transfer	1D, 1D axisymmetric, 2D, 2D axisymmetric, 3D
Temperature	0D
Solid Mechanics	1D, 1D axisymmetric, 2D, 2D axisymmetric, 3D
Advanced	0D, 1D, 1D axisymmetric, 2D, 2D axisymmetric, 3D
Discretization	1D, 1D axisymmetric, 2D, 2D axisymmetric, 3D

When the Metal Phase Transformation interface is added, three nodes are also added to the **Model Builder** — two **Metallurgical Phase** nodes and one **Phase Transformation** node. The phase transformation node will be set to use the two metallurgical phases as source and destination phases, respectively. From the **Physics** toolbar, you can add additional metallurgical phases and phase transformations. You can also right-click **Metal Phase Transformation** to select physics features from the context menu.

SETTINGS

The **Label** is the default physics interface name.

The **Name** is used primarily as a scope prefix for variables defined by the physics interface. Refer to such physics interface variables in expressions using the pattern `<name>.<variable_name>`. In order to distinguish between variables belonging to

different physics interfaces, the `name` string must be unique. Only letters, numbers, and underscores (_) are permitted in the **Name** field. The first character must be a letter.

The default **Name** (for the first physics interface in the model) is `metp`.

MATERIAL PROPERTIES

You have the option of letting the physics interface compute effective thermal, electromagnetic, and mechanical material properties, based on the corresponding properties and fractions of the individual metallurgical phases. Select the **Compute effective material properties** checkbox (selected by default) to let the physics interface compute effective thermal, electromagnetic, and mechanical material properties. You can use the computed effective material properties to create a compound material that can be used in other physics interfaces as a domain material. Select the **Create Compound Material** to create a compound material. This material is created at the component level. It will hold material properties corresponding to the settings in the physics interface.

HEAT TRANSFER

Phase transformations are inherently temperature dependent. Select the temperature field to use from the **Temperature** list. If you want to consider the release or absorption of latent heat during phase transformations, select the **Enable phase transformation latent heat** checkbox. You can then define values for the latent heat at each of the phase transformation nodes. By default, the checkbox is not selected.

TEMPERATURE

Phase transformations are inherently temperature dependent. Enter an expression for the temperature to use. To emulate the conditions of a dilatometry experiment, you can calculate thermal strains that result from the changing temperature and from phase transformations that take place. Select **Enable thermal strains** to enable the calculation of thermal strains, and select a **Thermal strain formulation — Strain based** or **Density based**. By default, the **Enable thermal strains** checkbox is not selected.

The two sections Heat Transfer and Temperature are mutually exclusive, and which one is active is determined by the space dimension.

SOLID MECHANICS

This section contains settings that affect various strains that accompany phase transformations. Select the **Enable phase plasticity** checkbox if you want to allow for

plasticity in the individual phases. Select the **Enable transformation-induced plasticity** checkbox if you want to include this type of transformation strain in your analysis. Select **Enable thermal strains** if you want to include thermal strains in your analysis. Note that the thermal strains will include both pure thermal strains as well as strains that arise from volumetric differences between different metallurgical phases. If you have selected **Enable thermal strains**, select a **Thermal strain formulation — Strain based** or **Density based**. By default, none of the three checkboxes in this section are selected. The **Enable phase plasticity** and **Enable thermal strains** checkboxes are visible only if you have selected the **Compute effective material properties** checkbox in the **Material Properties** section.

ADVANCED

By default, bounds for computed phase fractions and their sum, are checked during a simulation. If you select **Advanced Physics Options**, the **Advanced** section is used to modify the bounds that are used, or to disable the bounds checking altogether. When you have selected **Check phase fraction bounds**, you can modify the:

- **Maximum phase fraction sum**, which defines the numerical upper bound for the phase fraction sum.
- **Minimum phase fraction sum**, which defines the numerical lower bound for the phase fraction sum.
- **Minimum phase fraction**, which defines the numerical lower bound for each phase fraction, individually.

Normally, you should let COMSOL Multiphysics perform bounds checking of the computed phase fractions. Modify the default bounds with care, to ensure a valid solution. Disabling the bounds checking altogether can be useful during model development, for example when implementing your own phase transformation model.

DISCRETIZATION

The discretization for phase fractions is set using the **Discretization for phase fractions** list. By default, **Linear** is selected.

!	Note that when you set the **Discretization for phase fractions** to Gauss-point data, spatial gradients of the phase fractions will not available. This can be relevant in other physics interfaces, should the gradients of phase fractions be required.

Metallurgical Phase

The **Metallurgical Phase** node defines a phase. Depending on the settings at the physics interface level and the space dimension where the physics interface is used, the phase node will contain different sections, see Table 4-2.

TABLE 4-2: METALLURGICAL PHASE SECTIONS.

SECTION	AVAILABILITY
Model Input	0D, 1D, 1D axisymmetric, 2D, 2D axisymmetric, 3D
Initial Phase Fraction	0D, 1D, 1D axisymmetric, 2D, 2D axisymmetric, 3D
Transformation Times	0D
Phase Material	0D, 1D, 1D axisymmetric, 2D, 2D axisymmetric, 3D
Heat Transfer Properties	1D, 1D axisymmetric, 2D, 2D axisymmetric, 3D
Electromagnetic Properties	2D, 2D axisymmetric, 3D
Mechanical Properties	1D, 1D axisymmetric, 2D, 2D axisymmetric, 3D
Material Properties	0D

MODEL INPUT

Provide the **Volume reference temperature** T_{ref} for the phase. For calculations of thermal strains using **Thermal strain formulation — Strain based**, selected at the physics interface level, it represents the temperature at which the thermal strain is zero for the phase. For **Thermal strain formulation — Density based** it represents the temperature at

which the density is at its reference value. This reference density, together with the initial phase fraction, is used to calculate the initial density of the compound material.

Note that for **Thermal strain formulation — Density based**, the **Volume reference temperature** T_{ref} should be equal across phases. Otherwise, the computed density of the compound material, and the resulting thermal strain, will be incorrect.

Select the **Equivalent plastic strain**, ε_{epe}, and the **Equivalent plastic strain rate**, $\dot{\varepsilon}_{\text{epe}}$, from the respective lists.

- Note that each phase computes its own equivalent plastic strain and corresponding rate. These will often coincide with the corresponding quantities in the Plasticity feature in Solid Mechanics. However, if the phase is used as **Destination phase** in a Phase Transformation node, and the **Plastic recovery** option is used, this is no longer true, and it becomes important to explicitly select the **Equivalent plastic strain** and **Equivalent plastic strain** computed by the phase.
- When the Metal Phase Transformation interface is added, every created phase will be configured automatically in this regard.

INITIAL PHASE FRACTION

Define the **Initial phase fraction** for the phase. This fraction should be a value between zero and one, and you have to ensure that the initial phase fractions for all the phases in your analysis sum to one.

- The initial fractions for the metallurgical phases are named `metp.phase1.xi0`, `metp.phase2.xi0`, and so on.
- The current phase fractions are correspondingly named `metp.phase1.xi` and `metp.phase2.xi`.

For results processing purposes, variables are used that produce smoother fields by internally using the `gpeval` operator. These are for example `metp.phase1.xi0Gp`, `metp.phase1.xiGp`, and so on.

TRANSFORMATION TIMES

If you select **Compute transformation times**, you can store the times $\hat{t}$ and temperatures $\hat{T}$ during an analysis, corresponding to reaching specified target phase fractions. Enter a list of **Target phase fractions** $\hat{\xi}$ in the table. Whether transformation times and temperatures are recorded depends on if the phase fraction is increasing or decreasing during the analysis. Select **Decreasing phase fraction** if the phase fraction is expected to reach the specified target values when it is decreasing. With **Compute transformation times** selected, and in the case a phase fraction is increasing over time, you can select **Compute time to completion**. Enter the **Completion rate**, that is, a rate of phase formation low enough that the formation of the phase can be considered complete.

If the second Target phase fraction in the table is reached for a Metallurgical Phase (`phase4`) in an Austenite Decomposition interface (`audc`), the corresponding transformation time and temperature will be `audc.phase4.time_2` and `audc.phase4.temperature_2`.

PHASE MATERIAL

From the **Phase material** list, you select the material that defines the material properties for the phase. This section is visible depending on specific selections at the physics interface level. For the 0D space dimension, the **Phase material list** is visible if the **Enable thermal strains** checkbox has been selected. For other space dimensions, it is visible only if at least one of the **Compute effective thermal properties**, the **Compute effective electromagnetic properties**, or the **Compute effective mechanical properties** checkboxes has been selected at the physics interface level. You can create a material at the component level by using **Create Phase Material**. When you define material properties for the phase, **From material** will refer to the material that you have selected from the **Phase material** list. The phase material will hold material properties corresponding to the settings in the physics interface.

HEAT TRANSFER PROPERTIES

If the **Compute effective material properties** has been selected at the physics interface level, you must define the thermal properties for the phase. The default **Thermal conductivity** k, **Density** ρ, and **Heat Capacity at constant pressure** C_p, use values **From material**. The **From material** option refers to the selected material from the **Phase Material** list. For **User defined**, enter values or expressions for these properties.

ELECTROMAGNETIC PROPERTIES

If the **Compute effective material properties** has been selected at the physics interface level, you must define electromagnetic properties for the phase. The default **Relative permeability** μ_r, **Electric conductivity** σ, and **Relative permittivity** ε_r, use values **From material**. The **From material** option refers to the selected material from the **Phase Material** list. For **User defined**, enter values or expressions for these properties.

MECHANICAL PROPERTIES

If the **Compute effective material properties** has been selected at the physics interface level, you must define mechanical properties for the phase. The default Young's modulus E and Poisson's ratio ν use values **From material**. For **User defined**, enter values or expressions for these properties.

If **Enable thermal strains** has been selected with **Thermal strain formulation — Strain based** at the physics interface level, you have to define the **Secant coefficient of thermal expansion** α for the phase. By default, the value is taken **From material**. For **User defined**, enter a value or expression.

If **Enable phase plasticity** has been selected at the physics interface level, you have to define the plastic behavior of the phase. The default **Initial yield stress** σ_{ys0} uses a value **From material**. For **User defined**, enter another value or expression for initial yield stress. Initial yield stresses for phases can be weighted differently. This is useful when initial yield stresses for the phases in the model are very different. Select a **Weight factor for yield stress** — **Linear**, **Geijselaers**, or **User defined**. If **Geijselaers** is selected, you also need to specify a **Soft phase**, which is considered plastically soft in comparison to this phase. You should typically use this to give a stronger weight to martensite (hard) in relation to austenite (soft).

Select the **Isotropic hardening model** — **Perfectly plastic**, **Linear**, or **User defined** to define the hardening behavior of the phase.

Linear

Specify the **Isotropic hardening modulus** E_{Tiso}. The default value is taken **From material**.

User defined

For **User defined**, enter another value or expression for the modulus. If a **User defined** isotropic hardening modulus is selected, you have to select the **Hardening function**. By default, the value is taken **From material**.

For **User defined**, enter a value or expression for the **hardening function**. The expression can depend, for example, on the equivalent plastic strain in the phase.

In a phase (`phase4`) of an Austenite Decomposition interface (`audc`), the equivalent plastic strain is `audc.phase4.epe`.

Phase Transformation

Depending on the settings at the physics interface level and the space dimension where the physics interface is used, the phase transformation node will contain different sections.

PHASE TRANSFORMATION

The phase transformation defines how one phase forms (the destination phase) at the expense of another (the source phase). Select **Source phase** ξ^{s} and **Destination phase** ξ^{d} from the list of defined phases. Select a **Phase transformation model** — **Leblond–Devaux**, **Johnson–Mehl–Avrami–Kolmogorov**, **Kirkaldy–Venugopalan, simplified**, **Microstructure based**, **Koistinen–Marburger**, **Hyperbolic rate**, or **User defined**.

Leblond–Devaux

Select a **Formulation** — **Time and equilibrium**, **General coefficients**, **TTT diagram data**, or **Parameterized TTT diagram**.

- For **Time and equilibrium**, select an **Equilibrium phase fraction** $\xi_{\mathrm{eq}}^{\mathrm{d}}$ from the list. For **User defined**, specify an expression for $\xi_{\mathrm{eq}}^{\mathrm{d}}$. Specify a **Time constant** $\tau_{\mathrm{s}\to\mathrm{d}}$.
- For **General coefficients**, specify the expressions for $K_{\mathrm{s}\to\mathrm{d}}$ and $L_{\mathrm{s}\to\mathrm{d}}$. For **TTT diagram data**, select an **Equilibrium phase fraction** $\xi_{\mathrm{eq}}^{\mathrm{d}}$ from the list. For **User defined**, specify an expression for $\xi_{\mathrm{eq}}^{\mathrm{d}}$. Specify the **Relative phase fraction** X_1, and the **Transformation time** t_1.
- For **Parameterized TTT diagram**, select an **Equilibrium phase fraction** $\xi_{\mathrm{eq}}^{\mathrm{d}}$ from the list. For **User defined**, specify an expression for $\xi_{\mathrm{eq}}^{\mathrm{d}}$. Specify the **Relative phase fraction** X_1. In the **TTT Curve I** section, specify the transformation times t_{L}, t_{N}, and t_{U} corresponding to points on the lower part, the "nose", and the upper part of the TTT curve at the relative phase fraction X_1. Specify the corresponding transformation temperatures T_{L}, T_{N}, and T_{U}, and the TTT curve shape parameters q_{NL} and q_{NU}.

If applicable, select **Define temperature limits**, and select the **Lower temperature limit** T_l and the **Upper temperature limit** T_u from the respective lists. For the **User defined** options, specify, respectively, expressions for T_l and T_u.

The **Equilibrium phase fraction**, **Lower temperature limit**, and **Upper temperature limit** lists used by phase transformation nodes are populated by values calculated by the Steel Composition node.

Johnson–Mehl–Avrami–Kolmogorov

Select a **Formulation** — **Time, equilibrium and exponent**, **TTT diagram data**, **TTT diagram data, fixed exponent**, **Parameterized TTT diagram**, or **Parameterized TTT diagram, fixed exponent**.

- For **Time, equilibrium and exponent**, select an **Equilibrium phase fraction** $\xi_\mathrm{eq}^\mathrm{d}$ from the list. For **User defined**, specify an expression for $\xi_\mathrm{eq}^\mathrm{d}$. Specify the **Time constant** $\tau_{\mathrm{s}\to\mathrm{d}}$, and the **Avrami exponent** $n_{\mathrm{s}\to\mathrm{d}}$.
- For **TTT diagram data**, select an **Equilibrium phase fraction** $\xi_\mathrm{eq}^\mathrm{d}$ from the list. For **User defined**, specify an expression for $\xi_\mathrm{eq}^\mathrm{d}$. Specify the **Relative phase fraction** X_1, the **Transformation time** t_1, the **Relative phase fraction** X_2, and the **Transformation time** t_2.
- For **TTT diagram data, fixed exponent**, select an **Equilibrium phase fraction** $\xi_\mathrm{eq}^\mathrm{d}$ from the list. For **User defined**, specify an expression for $\xi_\mathrm{eq}^\mathrm{d}$. Specify the **Avrami exponent** $n_{\mathrm{s}\to\mathrm{d}}$, the **Relative phase fraction** X_1, and the **Transformation time** t_1.
- For **Parameterized TTT diagram**, select an **Equilibrium phase fraction** $\xi_\mathrm{eq}^\mathrm{d}$ from the list. For **User defined**, specify an expression for $\xi_\mathrm{eq}^\mathrm{d}$. Specify the **Relative phase fraction** X_1, and the **Relative phase fraction** X_2. In the **TTT Curve 1** section, specify the transformation times t_L, t_N, and t_U corresponding to points on the lower part, the "nose", and the upper part of the TTT curve at the **Relative phase fraction** X_1. Specify the corresponding transformation temperatures T_L, T_N, and T_U, and the TTT curve shape parameters q_NL and q_NU. In the **TTT Curve 2** section, specify the parameters for the TTT curve at the **Relative phase fraction** X_2.
- For **Parameterized TTT diagram, fixed exponent**, select an **Equilibrium phase fraction** $\xi_\mathrm{eq}^\mathrm{d}$ from the list. For **User defined**, specify an expression for $\xi_\mathrm{eq}^\mathrm{d}$. Specify the **Avrami exponent** $n_{\mathrm{s}\to\mathrm{d}}$, and the **Relative phase fraction** X_1. In the **TTT Curve 1** section, specify the transformation times t_L, t_N, and t_U corresponding to points on the lower part, the "nose", and the upper part of the TTT curve at the **Relative phase fraction** X_1. Specify the corresponding transformation temperatures T_L, T_N, and T_U, and the TTT curve shape parameters q_NL and q_NU.

If the rate term in the phase transformation model is to account for a nonzero initial phase fraction of the source phase, select **Include effect of initial phase fraction**. If applicable, select **Define temperature limits**, and select the **Lower temperature limit** T_l and the **Upper temperature limit** T_u from the respective lists. For the **User defined** options, specify, respectively, expressions for T_l and T_u.

Kirkaldy–Venugopalan, simplified

Select a **Formulation** — **Rate coefficient**, **TTT diagram data**, or **Parameterized TTT diagram**.

- For **Rate coefficient**, select an **Equilibrium phase fraction** $\xi_\mathrm{eq}^\mathrm{d}$ from the list. For **User defined**, specify an expression for $\xi_\mathrm{eq}^\mathrm{d}$. Specify the **Reference rate** $\dot{\xi}_0^\mathrm{d}$.
- For **TTT diagram data**, select an **Equilibrium phase fraction** $\xi_\mathrm{eq}^\mathrm{d}$ from the list. For **User defined**, specify an expression for $\xi_\mathrm{eq}^\mathrm{d}$. Specify the **Relative phase fraction** X_1, and the **Transformation time** t_1.
- For **Parameterized TTT diagram**, select an **Equilibrium phase fraction** $\xi_\mathrm{eq}^\mathrm{d}$ from the list. For **User defined**, specify an expression for $\xi_\mathrm{eq}^\mathrm{d}$. Specify the **Relative phase fraction** X_1. In the **TTT Curve 1** section, specify the transformation times t_L, t_N, and t_U corresponding to points on the lower part, the "nose", and the upper part of the TTT curve at the relative phase fraction X_1. Specify the corresponding transformation temperatures T_L, T_N, and T_U, and the TTT curve shape parameters q_NL and q_NU.

The rate term can be modified from its original form. If applicable, select **Include retardation term**, and specify the **Retardation coefficient** C_r. If applicable, select **Define temperature limits**, and select the **Lower temperature limit** T_l and the **Upper temperature limit** T_u from the respective lists. For the **User defined** options, specify, respectively, expressions for T_l and T_u.

Microstructure based

Select an **Equilibrium phase fraction** $\xi_\mathrm{eq}^\mathrm{d}$ from the list. For **User defined**, specify an expression for $\xi_\mathrm{eq}^\mathrm{d}$. Select a **Phase transformation function** f from the list. For **User defined**, specify an expression for f. Select a **Rate exponent** a from the list. Select an **Undercooling exponent** m from the list. Select the **Lower temperature limit** T_l and the **Upper temperature limit** T_u from the respective lists.

The rate term can be modified from its original form. If applicable, select **Include retardation term**, and select a **Retardation coefficient** C_r from the list. For **User defined**, specify an expression for C_r.

Koistinen–Marburger

Select a **Formulation** — **Koistinen–Marburger coefficient** or **Martensite finish temperature**.

- For **Koistinen–Marburger coefficient**, specify the **Martensite start temperature** M_s and, if applicable, select **Stress-dependent start temperature**. Specify the **Koistinen–Marburger coefficient** β.
- For **Martensite finish temperature**, specify the **Martensite start temperature** M_s and, if applicable, select **Stress-dependent start temperature**. Specify the **Martensite finish temperature** M_{90}.

If **Stress-dependent start temperature** has been selected, you have to specify how stresses affect the **Martensite start temperature** M_s.

- For the 0D space dimension, specify expression for the pressure p and the effective stress σ_e directly. Then specify the coefficients a_1 and a_2.
- For other space dimensions, you can select the pressure p and the effective stress σ_e from their respective lists. For the **User defined** options, specify expressions for these quantities directly. Then specify the coefficients a_1 and a_2.

If **Incomplete transformation** has been selected, specify the **Minimum retained source phase fraction** ξ_{ret}^{s}.

Hyperbolic rate

Specify the **Hyperbolic rate constant** $P_{s \to d}$ and select an **Equilibrium phase fraction** ξ_{eq}^{d} from the list. For **User defined**, specify an expression for ξ_{eq}^{d}. If applicable, select **Define temperature limits**, and select the **Lower temperature limit** T_l and the **Upper temperature limit** T_u from the respective lists. For the **User defined** options, specify, respectively, expressions for T_l and T_u.

Linear

Specify the **Lower temperature limit** T_l and the **Upper temperature limit** T_u from the respective lists. For the **User defined** options, specify, respectively, expressions for T_l and T_u.

Oddy–McDill–Karlsson

Specify the **Eutectoid austenite fraction** ξ_{eu}^{d} from the list. For **User defined**, specify an expression for ξ_{eu}^{d}. Under the **Time parameter** section, specify q_1 and q_2, and then specify the **Avrami exponent** $n_{s \to d}$. Specify the **Lower temperature limit** T_l and the **Upper temperature limit** T_u from the respective lists. For the **User defined** options, specify, respectively, expressions for T_l and T_u.

User defined

Specify the **Phase transformation contribution** $A_{s \to d}$. The expression defines the rate at which the destination phase forms, at the expense of the source phase.

If applicable, select **Define temperature limits**, and select the **Lower temperature limit** T_l and the **Upper temperature limit** T_u from the respective lists. For the **User defined** options, specify, respectively, expressions for T_l and T_u.

PHASE TRANSFORMATION LATENT HEAT

This section is active if you have selected **Enable phase transformation latent heat** at the physics interface level. You can specify the latent heat $\Delta H_{s \to d}$ that is released during the phase transformation.

PHASE TRANSFORMATION STRAIN

The **Transformation-induced plasticity** checkbox is available if you have selected **Enable transformation-induced plasticity** at the physics interface level. In case of transformation-induced plasticity, select **Transformation-induced-plasticity parameter** — **Thermal strain based** or **User defined**. The **Thermal strain based** option is available if **Enable phase plasticity** and **Enable thermal strains** have been selected at the physics interface level. For **User defined**, enter a value or an expression for the transformation-induced-plasticity parameter $K_{s \to d}^{TRIP}$ directly. Select the **Saturation function** Φ — **Abrassart**, **Desalos**, **Leblond**, **Tanaka**, or **User defined**. For **User defined**, enter an expression for the derivative of the saturation function.

The **Plastic recovery for destination phase** checkbox is available if the **Enable thermal strains** has been selected at the physics interface level. If you have selected **Plastic recovery** for destination phase, you can specify the **Plastic memory coefficient** $\Theta_{s \to d}$. The default value is zero, which means that no plastic straining in the source phase will be carried over to the destination phase.

If you have selected **Parameterized TTT Diagram** or **Parameterized TTT Diagram, Fixed Exponent**, you can visualize the TTT curve corresponding to the entered parameters in the **TTT curve 1** or **TTT Curve 2** sections.

- Make a preview plot by selecting **TTT curve preview**.
- Generate a plot by selecting **Create TTT curve plot**.

ADVANCED

Numerical smoothing can be applied at temperatures that correspond to a sudden activation or deactivation of the phase transformation. If you select **Advanced Physics Options**, the **Advanced** section is used to assign smoothing:

- **Transformation temperature smoothing**, ΔT, in case you have used **Define temperature limits**.
- **Martensite start temperature smoothing**, ΔM_s, in the case of the **Koistinen–Marburger** phase transformation model.

The smoothing parameters ΔT and ΔM_s each defines a temperature span across which the phase transformation rate term is smoothly ramped. In the limit of a zero smoothing parameter value, the ramping reduces to a Heaviside step function.

Transformation Condition

One or several **Transformation Condition** subnodes can be added to a **Phase Transformation node**. In the **Transformation Condition** subnode, specify a Boolean expression c that has to be satisfied for the **Phase Transformation** to take place. For example, if you have reason to prevent a phase transformation from occurring unless the temperature rate is negative, the expression could look like:

```
metp.Tt<0[K/s]
```

If several **Transformation Condition** subnodes are used, each separate condition has to be satisfied for the **Phase Transformation** to take place.

In some situations, a Boolean expression c may be numerically challenging. It can be beneficial to use smoothed transformation condition. For example, a general Boolean expression $a > b$ can be replaced by a smoothed Heaviside function as

```
flc1hs(2*(a-b)/h, 1)
```

causing c to increase smoothly from zero to one, across an interval of length h, centered at $a = b$.

Additional Source Phase

One or several **Additional Source Phase** subnodes can be added to a **Phase Transformation** node. In the **Additional Source Phase** subnode, select a metallurgical phase that

contributes to the formation of the **Destination phase** defined in the **Phase Transformation** node.

Steel Composition

The **Steel Composition** node is used to specify the chemical composition of a steel in terms of weight percentages of its alloying elements. Different empirical relationships are then used to establish characteristic transformation temperatures to be used in phase transformation modeling. In addition, the equilibrium phase fractions of metallurgical phases are computed as functions of temperature.

STEEL COMPOSITION

In the table **Weight percent of alloying elements**, specify the weight percentage (wt%) of each alloying element. For example, type 0.4 for **Carbon** for a steel with 0.4 percent carbon by weight (wt%).

DEFINITIONS

This section is used to specify the particular models used to compute composition-dependent phase transformation temperatures.

- Under **Ae1 and Ae3 temperatures**, specify how to model the A_{e1} and A_{e3} lines of an iron–carbon (Fe–C) diagram. If **Andrews** is selected, (constant) A_{e1} and (nonlinear) A_{e3} temperature lines are computed using empirical relationships based on the specified alloying content of the steel. If **Parameterized** is selected, (constant) A_{e1} and (linear) A_{e3} temperature lines are given in terms of three characteristic values. Specify the carbon concentration at the eutectoid, C^{γ}_{eut}. Select **Upper Ae3 temperature** to give the A_{e3} temperature at zero carbon concentration, A^{0}_{e3}, or select **Ae3** to specify A_{e3} directly. Specify the A_{e1} temperature.
- Under **Bainite start temperatures**, specify how to model the bainite start temperature. Select **Steven–Haynes Bs** or **Kirkaldy–Venugopalan Bs**.
- Under **Martensite start temperatures**, specify how to model the martensite start temperature. Select **Andrews Ms** or **Steven–Haynes Ms**.

Transformation Temperatures

Select **Calculate equilibrium phase fractions** to compute the equilibrium phase fraction of ferrite, as well as equilibrium phase fractions for pearlite and bainite. Select **Define**

phase transformation functions to enable the definition of functions used by the **Microstructure based** phase transformation model.

EQUILIBRIUM PHASE FRACTIONS

This section is available if **Calculate equilibrium phase fractions** has been selected. Specify the maximum ferrite solubility (at the eutectoid temperature), $C^{\alpha}_{\max}$. Under **Ferrite formation below the eutectoid**, specify how ferrite is formed below the temperature A_{e1}. Select **None** to set the ferrite equilibrium phase fraction to zero below the eutectoid (no formation of free ferrite). Select **Constant** to set the ferrite equilibrium phase fraction below the eutectoid equal to that at the eutectoid temperature. Select **Hultgren extrapolation** to model the ferrite equilibrium phase fraction based on the linear extrapolation method by Hultgren. For **Hultgren extrapolation**, specify the lowest temperature of the ferrite region in the Fe–C diagram, T^{α}_{0}, and the lowest temperature for the formation of free ferrite, T_C.

Equilibrium Phase Fractions

PHASE TRANSFORMATION MODELING

This section is available if **Define phase transformation functions** has been selected. It is used to define functions that become available to the **Microstructure based** phase transformation model in the **Phase transformation** node. Specify an expression for the **ASTM grain size number** G^{ASTM}. Select a **Phase transformation model formulation**—**Kirkaldy–Venugopalan** or **Li–Niebuhr–Meekisho–Atteridge**. For **Kirkaldy–Venugopalan**, the phase transformation functions can be modified to account for the presence of boron. Select **Åkerström–Oldenburg modification for boron steel**, and then under **Weight percent of boron**, enter an expression for wt%B.

Hardness

The **Hardness** subnode is used to compute the Vickers hardness (HV) and the Rockwell C hardness (HRC) of steel, after cooling from an austenitic state. One or several **Hardness** subnodes can be added to a **Steel Composition** node. In the **Hardness** subnode, you select the metallurgical phases that represent, respectively, ferrite, pearlite, bainite, and martensite. Based on this information, the chemical composition of the steel

defined in the parent **Steel Composition** node, and certain characteristics of the cooling transient, the hardness is computed.

	Hardness

5

Austenite Decomposition

This chapter describes the three Austenite Decomposition interfaces ( ) and their functionality. The interfaces are added from the **Heat Transfer** > **Metal Processing** branch ( ), and they are the **Austenite Decomposition**, the **Austenite Decomposition, Kirkaldy–Venugopalan**, and the **Austenite Decomposition, Li–Niebuhr–Meekisho–Atteridge** interfaces.

The Austenite Decomposition Interface

The **Austenite Decomposition** interface ( ) is found under the **Heat Transfer** > **Metal Processing** ( ) branch when adding a physics interface. The physics interface is intended for studying metallurgical phase transformations. You can use this interface to study diffusional, displacive, and user-defined (solid–solid) phase transformations. Physical phenomena, such as latent heat of phase transformation and transformation strains can be computed and used in Heat Transfer in Solids and Solid Mechanics. With the Nonlinear Structural Materials Module or the Geomechanics Module, plastic strains and hardening behavior of each metallurgical phase can be used in Solid Mechanics.

This interface is based on the Metal Phase Transformation interface. This chapter will only describe the nodes and settings that set the Austenite Decomposition interface apart from the Metal Phase Transformation interface. With regard to other settings at the physics interface level and feature level, see The Metal Phase Transformation Interface.

When the Austenite Decomposition interface is added, nine nodes are added to the **Model Builder** — five Metallurgical Phase nodes and four Phase Transformation nodes. The interface is tailored specifically to the decomposition of austenite into a combination of ferrite, pearlite, bainite, and martensite. The phase nodes are given names to reflect this:

- Austenite
- Ferrite
- Pearlite
- Bainite
- Martensite

The **Initial Phase Fraction** is set to one in the **Austenite** node, and zero in the other metallurgical phase nodes. Four **Phase Transformation** nodes are also created to define the relevant phase transformations:

- Austenite to Ferrite
- Austenite to Pearlite

- Austenite to Bainite
- Austenite to Martensite

The source and destination phases in each phase transformation are set to the corresponding phases that have been created. The **Phase transformation model** is set to **Leblond–Devaux** with **General coefficients**, except in **Austenite to Martensite**, where it is set to **Koistinen–Marburger**. The phase transformations of austenite into ferrite, pearlite, and bainite are only suitable for isothermal or cooling situations. Therefore, **Transformation condition** nodes are added to these **Phase transformation** nodes to limit them. The martensitic phase transformation is only active during cooling, by design.

A **Parameters** node is automatically created under **Global Definitions**. This node contains parameters for certain user inputs of the physics interface nodes.

From the **Physics** toolbar, you can delete or disable metallurgical phases and phase transformations that are irrelevant in a given situation, and you can add additional metallurgical phases and phase transformations. You can also right-click **Austenite Decomposition** to select physics features from the context menu.

SETTINGS

The **Label** is the default physics interface name.

The **Name** is used primarily as a scope prefix for variables defined by the physics interface. Refer to such physics interface variables in expressions using the pattern `<name>.<variable_name>`. In order to distinguish between variables belonging to different physics interfaces, the `name` string must be unique. Only letters, numbers, and underscores (_) are permitted in the **Name** field. The first character must be a letter.

The default **Name** (for the first physics interface in the model) is `audc`.

The Austenite Decomposition, Kirkaldy–Venugopalan Interface

The **Austenite Decomposition, Kirkaldy–Venugopalan** interface ( ) is found under the **Heat Transfer** > **Metal Processing** ( ) branch when adding a physics interface. The physics interface is intended for studying metallurgical phase transformations. The interface specifically uses the phase transformation modeling framework of Kirkaldy and Venugopalan, in which austenite decomposition into different destination phases is expressed in terms of, for example, grain size and chemical composition. Physical phenomena, such as latent heat of phase transformation and transformation strains can be computed and used in Heat Transfer in Solids and Solid Mechanics. With the Nonlinear Structural Materials Module or the Geomechanics Module, plastic strains and hardening behavior of each metallurgical phase can be used in Solid Mechanics.

When the Austenite Decomposition, Kirkaldy–Venugopalan interface is added, ten nodes are added to the **Model Builder** — five Metallurgical Phase nodes, four Phase Transformation nodes, and one Steel Composition node. The interface is tailored specifically to the decomposition of austenite into a combination of ferrite, pearlite, and bainite, using the phase transformation framework of Kirkaldy and Venugopalan. The displacive martensitic phase transformation is modeled using the Koistinen–Marburger phase transformation model. The **Steel Composition** node is added to the interface, and it is configured to compute:

- Start temperatures A_{e3}, A_{e1}, B_s, and M_s used by Kirkaldy and Venugopalan
- Equilibrium phase fractions for ferrite, pearlite, and bainite
- Phase transformation functions according to Kirkaldy and Venugopalan

You need to supply the chemical composition and the ASTM grain size number to the **Steel Composition** node.

The created phase nodes are given the following names:

- Austenite
- Ferrite
- Pearlite
- Bainite
- Martensite

The **Initial Phase Fraction** is set to one in the **Austenite** node, and zero in the other metallurgical phase nodes. Four **Phase Transformation** nodes are also created to define the relevant phase transformations:

- Austenite to Ferrite
- Austenite to Pearlite
- Austenite to Bainite
- Austenite to Martensite

The source and destination phases in each phase transformation are set to the corresponding phases that have been created. The **Phase transformation model** is set to **Microstructure based**, except in **Austenite to Martensite**, where it is set to **Koistinen–Marburger**. The phase transformation nodes are automatically configured to use temperature limits and phase transformation functions, as computed by the **Steel Composition** node.

From the **Physics** toolbar, you can delete or disable metallurgical phases and phase transformations that are irrelevant in a given situation, and you can add additional metallurgical phases and phase transformations. You can also right-click **Austenite Decomposition, Kirkaldy–Venugopalan** to select physics features from the context menu.

SETTINGS

The **Label** is the default physics interface name.

The **Name** is used primarily as a scope prefix for variables defined by the physics interface. Refer to such physics interface variables in expressions using the pattern `<name>.<variable_name>`. In order to distinguish between variables belonging to different physics interfaces, the `name` string must be unique. Only letters, numbers, and underscores (_) are permitted in the **Name** field. The first character must be a letter.

The default **Name** (for the first physics interface in the model) is `audc`.

The Austenite Decomposition, Li–Niebuhr–Meekisho–Atteridge Interface

The **Austenite Decomposition, Li–Niebuhr–Meekisho–Atteridge** interface ( ) is found under the **Heat Transfer** > **Metal Processing** ( ) branch when adding a physics interface. This interface is analogous to The Austenite Decomposition, Kirkaldy–Venugopalan Interface, except that it configures created nodes to with respect to the phase transformation modeling framework of Li, Niebuhr, Meekisho, and Atteridge, which draws upon and modifies the framework of Kirkaldy and Venugopalan.

SETTINGS

The **Label** is the default physics interface name.

The **Name** is used primarily as a scope prefix for variables defined by the physics interface. Refer to such physics interface variables in expressions using the pattern `<name>.<variable_name>`. In order to distinguish between variables belonging to different physics interfaces, the `name` string must be unique. Only letters, numbers, and underscores (_) are permitted in the **Name** field. The first character must be a letter.

The default **Name** (for the first physics interface in the model) is `audc`.

6

Alpha–Beta Phase Transformation

This chapter describes the Alpha–Beta Phase Transformation Interface ( ) and its functionality. It is found under the **Heat Transfer** > **Metal Processing** branch ( ) when adding a physics interface.

The Alpha–Beta Phase Transformation Interface

The **Alpha–Beta Phase Transformation** interface ( ) is found under the **Heat Transfer** > **Metal Processing** ( ) branch when adding a physics interface. The physics interface is intended for studying metallurgical phase transformations in α–β titanium alloys. You can use this interface to study diffusional, displacive, and user-defined (solid-solid) phase transformations. Physical phenomena, such as latent heat of phase transformation and transformation strains can be computed and used in Heat Transfer in Solids and Solid Mechanics. With the Nonlinear Structural Materials Module or the Geomechanics Module, plastic strains and hardening behavior of each metallurgical phase can be used in Solid Mechanics.

This interface is based on the Metal Phase Transformation interface. This chapter will only describe the nodes and settings that set the Alpha–Beta Phase Transformation interface apart from the Metal Phase Transformation interface. With regard to other settings at the physics interface level and feature level, see The Metal Phase Transformation Interface.

When the Alpha–Beta Phase Transformation interface is added, several nodes are added to the **Model Builder** — three Metallurgical Phase nodes and seven Phase Transformation nodes. The interface is tailored specifically to the phase transformations that can take place in α–β titanium alloys like Ti–6Al–4V. The Alpha–Beta Phase Transformation interface defines three major phases, whose node names are:

- Beta
- Widmanstätten Alpha
- Martensitic Alpha

	Phase transformation modeling of α–β titanium alloys sometimes includes an alpha phase that forms at the beta grain boundaries. This alpha phase is omitted here, as it often exists in small fractions. Should this level of modeling detail be warranted, additional metallurgical phase and phase transformation nodes can be added to the interface.

The **Initial Phase Fraction** is set to 0.11 in the **Beta** node, and 0.89 in the **Widmanstätten Alpha** node. These initial phase fractions are approximate values corresponding to an α–β titanium alloy like Ti–6Al–4V, at room temperature. Seven **Phase Transformation** nodes are also created to define the relevant phase transformations:

- Beta to Widmanstätten Alpha. This phase transformation is active under isothermal or cooling conditions, and it is active provided that the fraction of beta phase exceeds its equilibrium value.
- Beta to Martensitic Alpha (Fast). This phase transformation is active under cooling conditions, when the cooling rate exceeds a certain threshold rate, and below the **Martensite start temperature**.
- Beta to Martensitic Alpha (Slow). This phase transformation is active under cooling conditions, when the cooling rate is lower than the threshold rate mentioned above, and below the **Martensite start temperature**. Under these conditions, the maximum fraction of formed Martensitic alpha is limited by the equilibrium value of beta phase.
- Alpha to Beta. This phase transformation is used to model the dissolution of Widmanstätten and Martensitic alpha, into beta phase. It is active under heating conditions, and when the temperature exceeds the so-called beta start temperature.
- Martensitic Alpha to Beta. This phase transformation represents the dissolution of Martensitic alpha into beta phase. It is active at temperatures above the martensite dissolution temperature. In this phase transformation, the beta phase strives toward its equilibrium value.
- Martensitic Alpha to Widmanstätten Alpha. This phase transformation represents the dissolution of Martensitic alpha into Widmanstätten alpha phase. It is active at temperatures above the martensite dissolution temperature. In this phase transformation, the Widmanstätten alpha phase strives toward its equilibrium value.
- Beta Re-Formation. This phase transformation represents a simplified description of complete dissolution of alpha phase. It is active when the temperature exceeds the beta transus.

A **Parameters** node is automatically created under **Global Definitions**. This node contains parameters for certain user inputs of the physics interface nodes. Generated parameters include default values for characteristic transformation temperatures, for the Martensitic alpha rate threshold, and so on.

From the **Physics** toolbar, you can delete or disable metallurgical phases and phase transformations that are irrelevant in a given situation, and you can add additional metallurgical phases and phase transformations. You can also right-click **Alpha–Beta Phase Transformation** to select physics features from the context menu.

For an example how to model phase transformation that occur during welding of a titanium plate, see *Welding of a Titanium Plate*: Application Library path **Metal_Processing_Module/Titanium_Phase_Transformations/welding_of_a_titanium_plate**.

SETTINGS

The **Label** is the default physics interface name.

The **Name** is used primarily as a scope prefix for variables defined by the physics interface. Refer to such physics interface variables in expressions using the pattern `<name>.<variable_name>`. In order to distinguish between variables belonging to different physics interfaces, the `name` string must be unique. Only letters, numbers, and underscores (_) are permitted in the **Name** field. The first character must be a letter.

The default **Name** (for the first physics interface in the model) is `abp`.

7

Carburization

This chapter describes the Carburization interface ( ) and its functionality. It is found under the **Heat Transfer** > **Metal Processing** branch ( ) when adding a physics interface.

The Carburization Interface

The **Carburization** interface ( ) is found under the **Heat Transfer** > **Metal Processing** ( ) branch when adding a physics interface. The physics interface is intended for modeling carburization processes during heat treatment. The carburization process is based on diffusion, and it is used to compute the evolving mass fraction of carbon when a component is exposed to a carbon rich atmosphere.

When the Carburization interface is added, three default nodes are added to the **Model Builder** — a **Carburization** node, an **Initial Values** node, and a **Zero Carbon Flux** node.

SETTINGS

The **Label** is the default physics interface name.

The **Name** is used primarily as a scope prefix for variables defined by the physics interface. Refer to such physics interface variables in expressions using the pattern `<name>.<variable_name>`. In order to distinguish between variables belonging to different physics interfaces, the `name` string must be unique. Only letters, numbers, and underscores (_) are permitted in the **Name** field. The first character must be a letter.

The default **Name** (for the first physics interface in the model) is `carb`.

TEMPERATURE

Carbon diffusion is inherently temperature dependent. Select the temperature field to use from the **Temperature** list.

CARBURIZING CYCLE

This section contains settings for the carburization process. Select the carbon potential model to use from the **Carbon potential model** list. Select **Boost-diffuse cycle** if you want to model a two-stage carburization process, where a boost stage is followed by a diffuse stage. Define the **Boost carbon potential** c_{boost}, the **Diffuse carbon potential** c_{diffuse}, and the **Boost period** t_{boost}. Select **User defined** if you want to use your own expression for the carbon potential of the carburization process. Define the **Carbon potential** c_{pot}.

Carburization

The Carburization node defines the carbon diffusion inside the domain.

CARBON DIFFUSION

From the **Diffusion coefficient** list you select the diffusion coefficient that is used in the diffusion equation. Select **Arrhenius** to define a thermally activated diffusion coefficient. Define the **Pre-exponential factor** D_0 and the **Activation energy** Q_D. Select **User defined** to define the **Diffusion coefficient** D directly.

Carbon Flux

The Carbon Flux node is used to define the carbon exchange with the surrounding carbon atmosphere (the exterior).

CARBON MASS TRANSFER

From the **Carbon potential list**, select the carbon potential of the exterior c_{ext}. Select **Carbon potential** to use the carbon potential defined at the physics interface level. Select **User defined** to define the carbon potential directly. From the **Mass transfer coefficient** list, select the mass transfer coefficient to be used to define the carbon flux. Select **Arrhenius** to define a thermally activated mass transfer coefficient. Define the **Pre-exponential factor** b_0 and the **Activation energy** Q_b. Select **User defined** to define the **Mass transfer coefficient** b directly.

Zero Carbon Flux

The Zero Carbon Flux node is used to define boundaries where no carbon exchange takes place with the exterior.

Carbon Concentration

The Carbon Concentration node is used to specify the carbon concentration at an exterior domain boundary.

CARBON CONCENTRATION

From the list, select the carbon concentration c_0. Select **Carbon potential** to use the carbon potential defined at the physics interface level. Select **User defined** to specify the carbon concentration c_0 directly.

Initial Values

The Initial Values node is used to specify the initial carbon concentration c.

8

Multiphysics Interfaces and Couplings

The Metal Processing Module contains predefined multiphysics interfaces to facilitate the coupling to Heat Transfer in Solids and Solid Mechanics interfaces. The physics interfaces are found under the **Heat Transfer** > **Metal Processing** branch ( ) when adding a physics interface — **Heat Transfer with Phase Transformations** and **Steel Quenching**. Two multiphysics coupling features — **Phase Transformation Latent Heat** and **Phase Transformation Strain**, can be added to facilitate the coupling to Heat Transfer in Solids and Solid Mechanics.

In this chapter:

Heat Transfer with Phase Transformations

The **Heat Transfer with Phase Transformations** multiphysics interface ( ) combines a Heat Transfer in Solids interface with a Metal Phase Transformation interface. When the Heat Transfer with Phase Transformations multiphysics interface is added, the multiphysics coupling **Phase Transformation Latent Heat** is included.

On the Constituent Physics Interfaces

- The Heat Transfer in Solids interface is described in The Heat Transfer in Solids Interface of the *Heat Transfer Module User's Guide*.
- The Metal Phase Transformation interface is described in The Metal Phase Transformation Interface chapter.

SETTINGS FOR PHYSICS INTERFACES AND COUPLING FEATURES

The **Enable phase transformation latent heat** checkbox is selected in the Metal Phase Transformation interface.

Steel Quenching

The **Steel Quenching** multiphysics interface ( ) combines a Heat Transfer in Solids interface with an Austenite Decomposition interface and a Solid Mechanics interface. When the Steel Quenching multiphysics interface is added, the **Phase Transformation Latent Heat** and **Phase Transformation Strain** multiphysics couplings are included.

On the Constituent Physics Interfaces

- The Heat Transfer in Solids interface is described in The Heat Transfer in Solids Interface of the *Heat Transfer Module User's Guide*.
- The Austenite Decomposition interface is described in The Austenite Decomposition Interface chapter.
- The Solid Mechanics interface is described in The Solid Mechanics Interface of the *Structural Mechanics Module User's Guide*.

SETTINGS FOR PHYSICS INTERFACES AND COUPLING FEATURES

The following checkboxes are selected in the Austenite Decomposition interface:

- Compute effective material properties
- Enable phase transformation latent heat
- Enable transformation-induced plasticity
- Enable thermal strains

The discretization for the temperature field in the Heat Transfer in Solids interface is set to Linear, because thermal strains are typically linear in the Solid Mechanics interface.

Induction Hardening

The **Induction Hardening** multiphysics interface ( ) combines a Heat Transfer in Solids interface with an Austenite Decomposition interface, a Solid Mechanics interface, and a Magnetic Fields interface. When the Induction Hardening multiphysics interface is added, the **Phase Transformation Latent Heat**, **Phase Transformation Strain**, and **Electromagnetic Heating** multiphysics couplings are included.

On the Constituent Physics Interfaces

- The Heat Transfer in Solids interface is described in The Heat Transfer in Solids Interface of the *Heat Transfer Module User's Guide*.
- The Austenite Decomposition interface is described in The Austenite Decomposition Interface chapter.
- The Solid Mechanics interface is described in The Solid Mechanics Interface of the *Structural Mechanics Module User's Guide*.
- The Magnetic Fields interface is described in The Magnetic Fields Interface of the *AC/DC Module User's Guide*.

SETTINGS FOR PHYSICS INTERFACES AND COUPLING FEATURES

The following checkboxes are selected in the Austenite Decomposition interface:

- Compute effective material properties
- Enable phase transformation latent heat
- Enable transformation-induced plasticity
- Enable thermal strains

The discretization for the temperature field in the Heat Transfer in Solids interface is set to Linear, because thermal strains are typically linear in the Solid Mechanics interface. The discretization for the magnetic vector potential in the Magnetic Fields interface is set to Linear, as this is often beneficial in induction hardening simulations. A **Coil** feature is automatically added to the Magnetic Fields interface.

Phase Transformation Latent Heat Multiphysics Coupling

The **Phase Transformation Latent Heat** multiphysics coupling ( ) is used to add the latent heat that is produced by a phase transformation physics interface as a heat source term in the heat equation of the coupled Heat Transfer in Solids interface. When the coupling is used, no separate Heat Source feature in the Heat Transfer interface is required.

When the **Phase Transformation Latent Heat** multiphysics coupling is used, the effect of latent heat should not be added as a **Heat Source** in the Heat Transfer in Solids interface, as this incorrectly amounts to adding the latent heat contribution twice.

SETTINGS

The **Label** is the default multiphysics coupling feature name.

The **Name** is used primarily as a scope prefix for variables defined by the coupling node. Refer to such variables in expressions using the pattern `<name>.<variable_name>`. In order to distinguish between variables belonging to different coupling nodes or physics interfaces, the `name` string must be unique. Only letters, numbers, and underscores (_) are permitted in the **Name** field. The first character must be a letter.

The default **Name** (for the first multiphysics coupling feature in the model) is `lht1`.

DOMAIN SELECTION

When the coupling is added, selected entities in the coupled Heat Transfer in Solids and Metal Phase Transformation interfaces are included by default.

COUPLED INTERFACES

This section defines the physics involved in the multiphysics coupling. The **Metal Phase Transformation** and **Heat Transfer** lists include all applicable physics interfaces.

The default values depend on how the coupling node is created.

- If the node is added from the **Physics** ribbon (Windows users), **Physics** contextual toolbar (Mac and Linux users), or context menu (all users), then the first physics interface of each type in the component is selected as the default.
- If it the node added automatically when a multiphysics interface is selected in the **Model Wizard** or **Add Physics** window, then the two participating physics interfaces are selected.

See also the Theory for Phase Transformation Latent Heat

Phase Transformation Strain Multiphysics Coupling

The Phase Transformation Strain multiphysics coupling ( ) is used to include phase transformation strains that are produced by a phase transformation physics interface as an inelastic strain contribution to the total strain in the Solid Mechanics interface.

Note that if **Enable thermal strains** has been selected at the **Metal Phase Transformation** interface level, thermal strain effects are included in the phase transformation strains. In this situation no **Thermal Expansion** coupling should be used between Solid Mechanics and Heat Transfer in Solids.

SETTINGS

The **Label** is the default multiphysics coupling feature name.

The **Name** is used primarily as a scope prefix for variables defined by the coupling node. Refer to such variables in expressions using the pattern `<name>.<variable_name>`. In order to distinguish between variables belonging to different coupling nodes or physics interfaces, the `name` string must be unique. Only letters, numbers, and underscores (_) are permitted in the **Name** field. The first character must be a letter.

The default **Name** (for the first multiphysics coupling feature in the model) is `ptstr1`.

DOMAIN SELECTION

When the coupling is added, selected entities in the coupled Solid Mechanics and Metal Phase Transformation interfaces are included by default.

COUPLED INTERFACES

This section defines the physics involved in the multiphysics coupling. The **Metal Phase Transformation** and **Solid Mechanics** lists include all applicable physics interfaces.

The default values depend on how the coupling node is created.

- If the node is added from the **Physics** ribbon (Windows users), **Physics** contextual toolbar (macOS and Linux users), or context menu (all users), then the first physics interface of each type in the component is selected as the default.
- If it the node added automatically when a multiphysics interface is selected in the **Model Wizard** or **Add Physics** window, then the two participating physics interfaces are selected.

See also the Theory for Phase Transformation Strains

TIME STEPPING FOR STRAINS

This section is used to specify how TRIP strains and plastic strain recovery are computed. Under **Method**, select **Local ODEs** or **Domain ODEs**. For **Local ODEs**, the TRIP strains and the plastic recovery are computed using state variable based local Newton iterations, and no additional degrees of freedom are added to the model. For **Domain ODEs**, the TRIP strains and the plastic recovery are computed using domain level ODEs, and corresponding degrees of freedom are added to the model.

ADVANCED SETTINGS

To enable this section, click the **Show More Options** button () and select **Show Advanced Physics Options** in the **Show More Options** dialog. The section is shown if the selected **Method** under **Time Stepping For Strains** is **Local ODEs**. Normally these settings do not need to be changed.

For the **Local ODEs** method, you can make the following settings:

- **Maximum number of local iterations**. This defines the maximum number of iterations of the Newton loop when solving the local strain equations.
- **Absolute tolerance**. This defines the absolute tolerance for convergence of the local strain equations. Convergence is judged based on the step size, that is, the size of the Newton correction, of each equation.
- **Relative tolerance**. This defines the relative tolerance for convergence of the local strain equations. Convergence is judged based on the step size, that is, the size of the Newton correction, of each equation.

Annealing

The Annealing subnode to the Phase Transformation Strain multiphysics coupling is used to specify an annealing temperature above which plastic hardening variables (equivalent plastic strains) are set to zero.

ANNEALING

Specify the **Annealing temperature**, T_a.

- The **Annealing** subnode can only be used with the **Local ODEs** method under **Time Stepping for Strains** of the parent multiphysics coupling.
- The **Annealing** subnode must be used in conjunction with **Annealing** subnodes to **Plasticity** nodes of the coupled **Solid Mechanics** interface. The selection of the former subnode must match the aggregate selection of the latter.

Index